Sl. No.	IIT Ropar List of Recent Publications with Abstract Coverage: January, 2026
A	**Book Chapter(s)**
1.	Advancing circular economy practices in manufacturing: Innovations and applications in sustainable production **A Kumar**…D Bharti - Hybrid Materials and Advanced Manufacturing: Book Chapter, 2026 **Abstract:** A novel approach to manufacturing and consumption, the circular economy guarantees long-term, sustainable growth. We can increase resource efficiency, decrease raw material consumption, and recover waste by recycling it or turning it into a new product thanks to the circular economy. Over the past ten years the circular economy has evolved into a new paradigm that aims to address the world's resource and environmental problems. This idea, which was centred on resource extraction and abandonment rather than sustainability, emerged in the late 20th century as a response to the rising awareness of the limitations of linear economic systems. Therefore, the circular economy's goal is to maximize our material resources by implementing the three fundamental principles of reduce, reuse, and recycle. In this approach, waste is utilized, product life cycles are prolonged, and a more sustainable and effective production model is developed over time. The concept stems from copying nature, where everything is valuable and exploited, and waste is transformed into new resources. This preserves the harmony between sustainability and progress. The research's conclusions will make it possible for partnerships to assist in overcoming these obstacles and advancing the circular economy as a workable industrial transformation paradigm.
2.	Assessing the pros and cons: Advantages and limitations of immobilized enzymes in practical applications **P Gangwar, H Yadav,** R Modi, M Garg - Recent Trends in Enzyme Immobilization: Book Chapter, 2026 **Abstract:** Enzymes immobilized, bound, or fixed in place, yet continuing to function and catalyze reactions, have revolutionized industrial and biotechnological processes. Immobilization improves enzyme reusability and cost-effectiveness while increasing resilience to environmental changes, such as harsh temperatures and pH levels. However, this technique presents certain obstacles, including potential activity loss during immobilization, mass transfer limits, and the necessity for careful selection of appropriate carriers and techniques customized to individual applications. This chapter critically evaluates the balance of these benefits and drawbacks, providing insights into industrial and medical uses and emphasizing their consequences for sustainability and efficiency.
3.	Biowaste as substrate for bioethanol production NK Shrivastava, AJ Siddiqa, PP Singh, **P Yadav,** S Verma - Energy Recovery from Organic Waste: Book Chapter, 2026 **Abstract:** The growing global demand for renewable energy has generated significant interest in bioethanol as a sustainable alternative to fossil fuels. One promising area for bioethanol production is the utilization of biowaste as a substrate. Biowaste, such as agricultural waste, food waste, and organic household waste, is an abundant and inexpensive feedstock for bioethanol production. This chapter explores the potential of biowaste as a substrate for bioethanol production and provides an in-depth look at different types of biowaste, their composition, and the pretreatment methods required to convert them into fermentable sugars. The chapter also discusses the role of microorganisms and enzymes in the fermentation process and focuses on recent advances in metabolic engineering and enzymatic technologies to improve bioethanol yields. Furthermore, the

	environmental and economic benefits of using biowaste for bioethanol production are discussed, with a focus on reducing greenhouse gas emissions and promoting a circular economy. Issues such as feedstock variability, efficiency of pretreatment, and process scalability are also discussed, along with potential solutions and future research directions. This chapter provides a comprehensive review of the state of the art in the technology of generating bioethanol from biowaste. It aims to inform researchers, policymakers, and industry players about the opportunities and challenges in the field, and ultimately contribute to the development of sustainable bioenergy solutions.
4.	Corrosion and radiation resistance properties of high entropy alloys T Talapaneni, **AL Kumar,** V Chaturvedi - Handbook of High Entropy Alloys: Book Chapter, 2025 **Abstract:** High-entropy alloys (HEAs) are a novel class of materials characterized by their multi-principal element compositions, which provide unique microstructures and remarkable mechanical, thermal, corrosion, and radiation resistance properties. This chapter comprehensively analyzes HEAs, focusing on their classification, processing methods, and phase formation while emphasizing their potential in demanding environments. The chapter explores the core effects of HEA composition, such as their influence on microstructure and material properties like hardness, wear resistance, fatigue strength, and thermal stability. The corrosion resistance of HEAs is examined through the lens of alloying elements and their impact in various environments, particularly resistance to chloride-induced and acidic corrosion. The corrosion testing methods, including potentiodynamic polarization and electrochemical impedance spectroscopy, are also thoroughly discussed. The radiation resistance of HEAs is another critical aspect, highlighted by their atomic arrangement, compositional complexity, and radiation-induced mechanical changes. Experimental techniques, including ion irradiation, positron annihilation spectroscopy, and atom probe tomography, are evaluated to understand HEAs' response to radiation. The synergistic effects of corrosion and radiation resistance, particularly in nuclear, aerospace, and defense applications, are analyzed to evaluate the impact of irradiation on corrosion behavior. Finally, this chapter explores the challenges and future directions in developing corrosion and radiation-resistant HEAs, emerging trends, and future research directions.
5.	Crop yield estimation with image fusion of scatterometer and multispectral data R Kaur, R Maini, **RK Tiwari** - Earth Observation using Scatterometers: Book Chapter, 2026 **Abstract:** Remote sensing has become a cost-efficient and effective way of estimating yield predictions due to the various advantages, such as simple data acquisition, data availability at a lower cost, global-level data acquisition, and multispectral or hyperspectral information. Additionally, it also allows crop health monitoring and the identification of diseases. Remote sensing acquires the Earth's surface data in various spectral bands, including the microwave region. However, the applicability of remote sensing is restricted due to various reasons, such as the presence of clouds in optical data and the limited resolution of microwave data. During the rainy season, it becomes challenging to monitor crop variations and other land cover types. Under this condition, microwave datasets are valuable because they have the potential to penetrate through the cloud. In this work, microwave and optical datasets are fused to develop cloud-free maps using the proposed framework, which integrates the features of nearest neighbour diffusion, neural networks and post-classification comparison. The primary objective of this work is to identify the soil moisture level, which acts as an important component of the crop yield estimation. The outcomes are generated with an accuracy of more than 92% in classification as well as change detection maps. This study allows the exploration of the potential of image fusion in the accurate development of classified and change maps for various potential applications.

6.	Food industry wastewater: An efficient bioorganic substrate to produce energy-rich microbial fuel cells AJ Siddiqa… **P Yadav** - Energy Recovery from Organic Waste: Book Chapter, 2026 **Abstract:** The food industry produces large volumes of organic-rich wastewater, representing both a waste management challenge and an opportunity for sustainable energy production. Microbial fuel cells (MFCs) have emerged as a promising technology to convert the organic components of food industry wastewater into electricity through microbial activity and harness their energy potential. This chapter describes food industry wastewater as a bioorganic substrate in MFCs, focusing on its composition, energy potential, and suitability for microbial degradation. The chapter outlines the fundamental principles of MFC operation, including the role of electroactive bacteria, electron-transfer mechanisms, and system configuration. It also discusses factors that affect MFC performance, including substrate concentration, pH, temperature, and electrode materials. Recent advances in MFC technology have been discussed, including genetically modified microorganisms and novel electrode designs that demonstrate the potential for enhanced energy recovery. Furthermore, the environmental and economic benefits of integrating MFCs into food-industry wastewater treatment processes, including reduced energy consumption and greenhouse gas emissions, are highlighted. Issues such as scalability, costs, and system optimization are discussed, as well as future research directions to overcome these barriers. By providing a comprehensive overview of this innovative approach, this chapter aims to stimulate further research and implementation of MFC technology for sustainable energy production and wastewater management in the food industry.
7.	Forecasting and tracking of natural hazards using scatterometers **N Mishra, D Iawphniaw, RK Tiwari** - Earth Observation using scatterometers: Book Chapter, 2026 **Abstract:** Scatterometers are active radar sensors mounted on satellites, aircraft, or fixed on the ground and are used in earth observation operating in the microwave spectrum. In this chapter, the different applications of scatterometry in oceanographic, geological, environmental, and meteorological hazards prediction and tracking are explored. Before scatterometers were launched, forecasting of natural disasters was done by means of instruments like anemometers, weather buoys, barometers, and visual observations. These methods have limited coverage and lower accuracy. The Seasat (Sea Satellite) was the first scatterometer satellite launched in 1978 to measure wind vectors over the ocean. From then onwards, advanced scatterometers operating at different bands of the microwave region were launched for forecasting and tracking hazards. Spaceborne scatterometers like Seasat and QuikSCAT (Quick Scatterometer) are mainly used for weather and climate forecasting. With higher resolution and operation at C-band and Ku-band, airborne scatterometers are mostly used for soil-moisture monitoring, ice mapping, and the advanced airborne scatterometers can also be used in climate monitoring and weather forecasting. Ground-based scatterometers can provide even finer spatial and temporal resolution due to their closer proximity to the target, so their continuous and high-resolution data are important for dynamic processes in the environment, and they can help in providing near real-time data for floods, earthquakes, and snow dynamics. This Chapter explains the revolution of the scatterometer for the Hazards Forecasting and Prediction of the Hazards.
8.	Life cycle assessment of eco-friendly fibers and polymers for the sustainable environment **A Sharma, M Rani, S Zafar, CK Nirala** - Eco-Friendly Fiber Reinforced Polymer Composite materials: Book Chapter, 2026 **Abstract:** The increasing global concern for environmental sustainability has prompted a surge in efforts to incorporate more eco-friendly materials into product design. A particularly promising

	approach involves utilizing natural fibers instead of synthetic ones as reinforcement materials in polymer composites. These efforts aim to reduce the environmental footprint associated with various stages of the product life cycle. Researchers have been actively investigating the potential benefits of natural fiber composites (NFCs) across various industries, including automotive, construction, and household appliances. One key method used to evaluate the environmental impact of NFCs is life cycle assessment (LCA). This offers a comprehensive analysis of the entire product life cycle, from raw material extraction to disposal. This chapter provides an overview of the LCA methodology and its applications in various NFC contexts. Additionally, it discusses the advantages and limitations of LCA in assessing NFCs and suggests future directions for research in this area.
9.	Machine learning models for crop monitoring from optical and microwave remote sensing R Kaur, R Maini, **RK Tiwari** - Earth Observation using Scatterometers: Book Chapter, 2026 **Abstract:** Crop monitoring is essential for maximising agricultural productivity, ensuring sustainability, and managing resources. Remote sensing allows the monitoring of crops at a large scale in a cost-effective way, even daily. Regular crop monitoring allows improved yield management, precision agriculture, and improved decision-making. However, the applicability of remote sensing data is affected due to many factors, such as the presence of clouds, atmospheric distortion, and limited availability. In this study, machine learning based classification has been performed on fused datasets using optical data from the Moderate Resolution Imaging Spectroradiometer and microwave data from SCATSAT-1. By combining these two datasets using nearest neighbour and classification using artificial neural network algorithms, the soil moisture data has been extracted for precise crop monitoring. Two classification algorithms, i.e., (1) random forest and (2) spectral angle mapper, have been implemented in this present study. The experimental results show that both classifiers provide satisfactory results with more than 90% accuracy in the classified maps. This study makes balanced and sustainable decisions for agriculture practices, while it also offers dependable information under different weather conditions, as well as the issues of cloud cover and limitations of the sensor. Future work includes the development and implementation of deep learning to improve performance and filter out potential errors in data gathering and analysis
10.	Retrieval of optical vegetation indices from SCATSAT-1 Ku-band backscatter: A comparative analysis with MODIS and Proba-V sensors DK Gupta… **S Singh, V Sood,** N Kumar - Earth Observation using Scatterometers: Book Chapter, 2026 Abstract: The extraction of vegetation indices from radar backscatter measurements offers a solution to optical remote sensing, especially in cloud-dominated areas where optical satellite observations are poor. This research explores the capability of Scatsat-1 Ku-band backscatter observations for normalised difference vegetation index (NDVI) estimation from two optical satellite instruments namely Moderate Resolution Imaging Spectroradiometer (MODIS) and Proba-V. Total of 60 different study sites are considered for taking the observations of Scatsat-1 backscattering coefficients and NDVI from two different sensors. A nonlinear statistical model has been developed for the retrieval of NDVI (MODIS and Proba-V) using Scatsat-1 backscattering coefficients at horizontal transmit, horizontal receive (HH) and vertical transmit, vertical receive (VV) polarisation by least square optimisation techniques. The validation results demonstrate that VV-polarised backscatter yields better NDVI retrieval accuracy than HH polarisation, with a higher correlation ($R = 0.796$) and lower root mean square error (RMSE) (0.058) for MODIS NDVI compared to $R = 0.579$ and RMSE = 0.057 for Proba-V NDVI. The bias values are near zero, showing no strong systematic overestimation or underestimation of the retrieval models. Yet, retrieval errors are more evident in low NDVI situations, where vegetation

	sparsity adds variability to backscatter response. The research validates that Scatsat-1 Ku-band backscatter data can be utilised to estimate NDVI effectively, offering an alternative for vegetation monitoring when optical sensors are obscured by cloud cover. Future studies need to investigate multi-temporal data fusion, machine learning methods, and other vegetation indices to further improve the accuracy and reliability of radar-based NDVI retrieval models.
11.	Thermochemical conversion of biomass to syngas via gasification **A Kumar,** TK Patra, **T Mondal** - Next-Generation Biofuels: Book Chapter, 2025 **Abstract:** The overconsumption of conventional fossil fuels by the energy and petrochemical sectors demands the development of an alternative renewable source. Biomass is an effective alternative renewable energy source for the carbon-neutral production of energy and chemicals. This chapter provides a comprehensive examination of constituents of biomass and biomass conversion technologies, specifically focusing on an overview of the gasification and pyrolysis processes used to convert biomass into gases, bio-oil, and biochar. Gasifier designs are generally categorized into downdraft, updraft, and fluidized beds. The selection of a specific gasifier type will depend on the end use and the quantity of the producer gas required. and its applications in energy generation and chemical synthesis.
B	**Conference Proceeding(s)**
12.	Assessment of collagen morphology in pancreatic tumor using computational translation of histological images **G Singhal, Nisha, G Uppal,** M Kaur, R Sinha, **R Kumar -** International Conference On Artificial Intelligence, Computing, IOT and Data Analytics, 2026 **Abstract:** Collagen remodeling is a hallmark of cancer progression and is critical for diagnosis and treatment planning. Second harmonic generation (SHG) microscopy, while effective for collagen imaging, is limited by high costs and the need for specialized equipment. In this study, we implemented a deep learning-based architecture to translate bright-field (BF) images of H&E-stained pancreatic tissue microarrays (TMAs) into the "collagen" images. The similarity analysis demonstrated that translated collagen images were equivalent to the SHG images. These translated images were subsequently used to extract collagen measures using first-order intensity-based texture analysis, which enabled the evaluation of morphological differences between tumor and normal pancreatic tissues. Statistical analysis was conducted to evaluate the significance of these collagen measures in distinguishing the classes. Furthermore, machine learning (ML) models were compared to identify the optimal model for differentiating the classes based on collagen measures. First-order intensity-based collagen measure analysis indicated "variance" as the most significant feature in classifying the two groups, which was in agreement with ROC-AUC (receiver operating characteristics–area under curve) analysis. The study indicated that the collagen features extracted from the "translated image" can be potentially used to understand the role of collagen remodeling in the progression of pancreatic tumors and can facilitate the analysis of stromal biomarkers.
13.	Machine learning model to study single-cell osteoarthritic chondrocytes via Raman spectroscopy **G Uppal, Nisha,** T Goyal, A Kumar, **R Kumar** - International Conference On Artificial Intelligence, Computing, IOT and Data Analytics, 2026 **Abstract:** Raman spectroscopy (RS) has become an imperative instrument in biomedical research. It is a nondestructive and label-free laser spectroscopic technique, which can identify chemical composition of a biological sample by detecting multiple molecular components simultaneously without the need or minimal sample preparation under physiological condition. A major limitation while analyzing Raman spectra of a biological sample is the overlapping nature of vibrational modes of different molecules at a single spectral peak. Machine learning (ML) techniques

	encompass various multivariate and statistical analysis methods, which can be broadly classified into supervised and unsupervised techniques. Multivariate curve resolution-alternating least square (MCR-ALS) technique is a multivariate ML model that can potentially deconvolute overlapping Raman vibrational modes and extract the meaningful spectra that can be associated with biochemical components along with their concentrations. In this study, Raman spectral data were acquired from osteoarthritic chondrocytes. The spectra of three cellular components associated with DNA, proteins, and lipids were extracted using MCR-ALS technique, and it was observed that concentration of DNA and proteins decreased while concentration of lipids increased with progression of osteoarthritic grades. The study indicated that combined approach of Raman-MCR analysis can open new possibilities for improved Raman spectral analysis, which might assist further in providing the meaningful interpretation of complex Raman spectra originated from the biological samples.
14.	Mapping optimal locations for artificial groundwater recharge using AHP-ANN and electrical resistivity survey **S Ganguly, T Prashanth, D Banerjee** - International conference on Mediterranean Geosciences Union, 2026 **Abstract:** Depletion of groundwater reserves has been designated as a serious problem all around the globe. Owing to rapid population growth, industrialization, and enhancement of living standards, the demand and exploitation of groundwater are rising at a rate larger than ever before. For instance, an estimate shows that the groundwater reserve in the north-western part of India depletes at a mean rate of 4.0 ± 1.0 cm/year, equivalent to a volume of 17.7 ± 4.0 km^3/year. Artificial groundwater recharge is a set of man-made techniques to replenish and augment the groundwater reserve at places where the natural recharge is not adequate. Artificial recharge structures (ARSs) are used to maintain a great balance between supply and demand. The primary goal of this study is to use the analytical hierarchy process (AHP) and feed-forward artificial neural network (ANN) to map locations appropriate for ARSs. Various factors, such as elevation, slope, drainage density, distance from the river, soil, land use and land cover, geomorphology, the thickness of shallow permeable layers, population distribution, and rainfall, are used to achieve the primary objective. The secondary goal is to map the subsurface using electrical resistivity tomography in order to detect an aquifer's depth range and overall geometry. To achieve the secondary goal, the apparent resistivity (Ohm-m) is calculated by using the Wenner–Schlumberger configuration, and the true resistivity (Ohm-m) of the subsurface is then calculated by using an inversion algorithm which solves Poisson's equation combined with Ohm's law using the Resistivity-2D Inversion (Res2DInv) software. The tertiary goal is to suggest an appropriate type of ARS by considering a number of variables, including the availability of water, land, cost, soil, lithology, geology, and geomorphology, as well as climate, topography, and land use. The sigmoid function is considered a transfer function inside the hidden layers of a forward-based ANN, and the weights are established by an iterative process so that the error between the observed and simulated data is tolerable. AHP relies on subjective expertise, whereas ANN is driven by data, producing superior results than AHP. Based on the analysis, we advise employing surface spreading techniques for users close to the Sutlej River. Injection well-type ARSs can be advised to the locations distant from rivers.
C	**Article(s)**
15.	A comparative study of Newtonian and multi-mode viscoelastic models for blood flow in stenosed arteries at high physiologic Reynolds and Womersley numbers **A Chauhan, C Sasmal** - International Journal of Engineering Science, 2026

	Abstract: This study presents extensive three-dimensional numerical simulations to investigate the hemodynamics within a stenosed artery under both steady and pulsatile inflow conditions. Two different blood rheology models are employed, namely, the conventional Newtonian model and the more physiologically accurate multimode simplified Phan–Thien–Tanner (sPTT) viscoelastic model. The parameters for the sPTT model are calibrated using experimental rheological data of real whole blood, obtained from standard viscometric flows such as steady simple shear and small-amplitude oscillatory shear (SAOS). This enables the model to capture both the shear-thinning and viscoelastic nature of blood, thus offering a more realistic representation of blood flow dynamics in a physiologically relevant arterial geometry. Under steady inflow conditions, a high-velocity jet is formed as blood flows through the stenosed region, which subsequently extends downstream into the post-stenotic area. This jet is found to be shorter in length but more turbulent and unsteady when simulated with the sPTT model compared to the Newtonian model. The sPTT model simulations reveal more concentrated small-scale vortical structures within and immediately downstream of the stenosis, indicating increased flow complexity due to viscoelastic and shear-thinning effects of blood. The same trend is also observed in the case of pulsatile flow conditions. Clinically significant hemodynamic parameters such as the pressure drop across the stenosis and wall shear stress (WSS) were also analyzed. The pressure drop is observed to decrease with increasing Reynolds number but increase with the degree of stenosis. WSS, a critical indicator in vascular health assessment, increases with stenosis severity and attains its maximum during the systolic (peak) phase of the pulsatile cycle, where blood velocity is at its highest. Throughout the simulations, the Newtonian model consistently overestimates both the pressure drop and WSS compared to the sPTT model. Therefore, reliance on Newtonian assumptions may lead to misinterpretation or overestimation of key hemodynamic metrics in both diagnostic and therapeutic contexts. Overall, this study provides in-depth insights into the complex flow behavior in stenosed arteries, with emphasis on the rheological fidelity of the blood model. The findings of this study have potential implications for improving clinical diagnosis, treatment planning, and the design of medical devices targeting vascular diseases in the context of atherosclerosis, a progressively prevalent cardiovascular condition.
16.	A critical assessment of measures of financing constraints: An application to Indian manufacturing **MA Vincent, S Bardhan,** PK Das - Journal of Quantitative Economics, 2026 **Abstract:** This paper critically evaluates the most commonly used measures of firm financing constraint, namely, the Kaplan and Zingales (KZ), Whited and Wu (WW), and Hadlock and Pierce (HP) indices, as well as the Stochastic Frontier Analysis (SFA), in the context of India. Using panel data on Indian manufacturing firms from the Prowess database for the period 1996–2019, the study constructs the KZ, WW, and HP indices based on firm balance sheet data, assuming parameter stability. We also employ SFA to quantify time-varying financing constraints. Correlation and panel regression analyses are used to compare the effectiveness of these measures. The findings reveal weak correlations among the selected measures, indicating that they capture distinct dimensions of financing constraints and classify firms differently. None of the approaches consistently identifies financially constrained firms across all the contexts considered. The analysis further offers alternative explanations for the observed patterns, highlighting the importance of a broader understanding of the factors influencing firm behaviour. By analysing India's distinct financial landscape, the paper underscores the need for a more refined approach to measuring financing constraints and offers valuable insights into firm-level financing dynamics.
17.	A provably secure lightweight three-factor 5G-AKA authentication protocol relying on an extendable output function **AK Yadav,** A Braeken, M Liyanage - IEEE Transactions on Network and Service Management, 2026

	Abstract: Compared to 4G, the designed authentication and key agreement protocol for 5G communication (5G-AKA) offers better security. State-of-the-art shows that various protocols indicate the flaws in the 5G-AKA and suggest solutions primarily for the desynchronization attack, traceability attack, and perfect forward secrecy. However, most authentication protocols fail to facilitate the device stolen attack and are expensive; they also do not consider the prominent security issues such as post-compromise security and non-repudiation. Considering the above demerits of these protocols and the necessity to offer additional security, a provably secure lightweight 5G-AKA multi-factor authentication protocol relying on an extendable output function is proposed. The security of the proposed work has been confirmed informally and formally (ROR logic, GNY logic, and Scyther tool) to ensure that the proposed work handles all types of attacks and offers additional security features, such as post-compromise features and non-repudiation. Furthermore, we compute the performance of the proposed work and compare it with its counterparts to show that our work is less costly and more suitable for lightweight devices than others in terms of computational, communication, storage, and energy consumption cost.
18.	A sustainable approach for synthesizing Mo2C MXene to reduce the wastage of gallium for energy storage devices P Kumar, A Bansal, **A Pandey,** V Chawla, **N Sardana,** R Chandra - Chemical Engineering Journal, 2026 **Abstract:** To promote sustainable MXene synthesis and minimize gallium consumption, we present an alternative approach utilizing the Mo_2GaC MAX phase by replacing the conventional Mo_2Ga_2C precursor. Mo_2CT_x MXene was synthesized using the traditional hydrofluoric acid etching, followed by delamination with tetrabutylammonium hydroxide. The freeze-dried MXene powder underwent comprehensive structural, surface, and chemical characterization techniques to confirm partial Ga removal. We subsequently studied the electrochemical energy storage capabilities of this partially etched MXene for supercapacitor applications. High-performance supercapacitor electrodes were fabricated through additive electrophoretic deposition, enabling the assembly of binder-free, rapid, and dense electrodes. Electrochemical performance was evaluated in Mo_2CT_x MXene//Li_2SO_4//graphite asymmetric configuration, demonstrating a volumetric capacitance of 175.4 F/cm^3 at a scan rate of 10 mV/s. The GCD analysis exhibited a high volumetric energy density of 14.7 mWh/cm^3 at a power density of 0.6 W/cm^3, with 78.2% storage retention over 10,000 cycles. These findings highlight the potential of Mo_2GaC as a viable and cost-effective precursor for the synthesis of Mo_2C. This also underscores the potential of additively manufactured, partially etched Mo_2CT_x MXene electrodes as a viable platform for the next-generation high-power-density thin film supercapacitors while simultaneously addressing material sustainability through reduced gallium wastage.
19.	A unified framework for EEG seizure detection using universum-integrated generalized eigenvalues proximal support vector machine **Y Kumar, V Ahire, M Ganaie** - Neural Networks, 2026 **Abstract:** The paper presents novel Universum-enhanced classifiers: the Universum Generalized Eigenvalue Proximal Support Vector Machine (U-GEPSVM) and the Improved U-GEPSVM (IU-GEPSVM) for EEG signal classification. Using the computational efficiency of generalized eigenvalue decomposition and the generalization benefits of Universum learning, the proposed models address critical challenges in EEG analysis: non-stationarity, low signal-to-noise ratio, and limited labeled data. U-GEPSVM extends the GEPSVM framework by incorporating Universum constraints through a ratio-based objective function, while IU-GEPSVM enhances stability through a weighted difference-based formulation that provides independent control over class separation and Universum alignment. The models are evaluated on the Bonn University EEG dataset across two binary classification tasks: (O vs S)-healthy (eyes closed) vs seizure, and (Z vs

	S)-healthy (eyes open) vs seizure. IU-GEPSVM achieves peak accuracies of 85% (O vs S) and 80% (Z vs S), with mean accuracies of 81.29% and 77.57% respectively, outperforming baseline methods. Rigorous statistical validation confirms these improvements: Friedman tests reveal significant overall differences, pairwise Wilcoxon signed-rank tests with Bonferroni correction establish IU-GEPSVM's superiority over all baselines, and win-tie-loss analysis demonstrates practical significance. Overall, integrating interictal Universum data yields an efficient and reliable solution for neurological diagnosis.
20.	A weighted monte Carlo method for modeling aggregation breakage phenomena: Application to Al2O3 nanoparticle aggregates **A Baid, K Ola,** S Bhoi, **J Kumar,** E Tsotsas - Powder Technology, 2026 **Abstract:** Simulating aggregation and breakage is challenging for broad particle size distributions with sparsely populated large-size classes. We develop a novel Weighted Monte Carlo (WMC) algorithm to simulate aggregation and breakage processes. This method offers significant advantages over the conventional Constant Number Monte Carlo (CNMC) algorithm, particularly in its ability to accurately capture size distributions and effectively represent particles that are fewer in number but larger in size. The algorithm's effectiveness has been validated through case studies involving breakage, aggregation, and their combination, demonstrating strong agreement with exact results. In the heavy-tailed test case for breakage, WMC reproduces both the volume distribution and the moments obtained from the Weighted Finite Volume Method, while CNMC shows clear deviations in the moments due to under-representation of the tail. Additionally, the new algorithm has been successfully applied to simulate the aggregation and breakage of nanoparticle aggregates in a spouted bed with a broad initial size distribution, accurately resolving the tail of the particle size spectrum. WMC also significantly reduces computational time, requiring 17 s compared to 5 h for CNMC in pure breakage, 28 s compared to 2 h in the heavy tailed breakage case and 208 s compared to 19 h for CNMC in pure aggregation, and 3 h in the experimental case where CNMC is not computationally feasible. 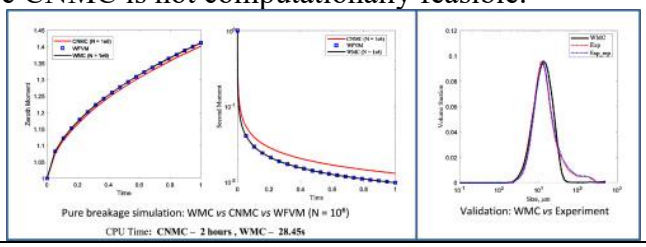
21.	Ablation resistance of metal/ceramic-infused polymer-based coating against high-energy laser **KK Pandey, V Kumar,** S Kaur, **E Ahmed, SW Khan,** S Rani, **R Kant,** A Nirwan, R Kumar, **H Singh**- Journal of Materials Science, 2026 **Abstract:** To address the growing threat of high-energy laser (HEL) attacks, this study focuses on developing phenolic resin-based composite coatings reinforced with various metallic and ceramic fillers. Among the formulations tested, the aluminum–molybdenum diboride ($Al + MoB_2$) composite coating exhibited the most promising laser ablation resistance. While pure aluminum displayed the highest reflectivity and alumina the lowest, the introduction of MoB_2 into the aluminum matrix significantly reduced reflectivity without compromising thermal performance. The $Al + MoB_2$ coating demonstrated the lowest backside temperature rise and minimal weight loss during laser exposure, indicating excellent thermal barrier characteristics and high resistance to material degradation. This superior performance is attributed to the high thermal stability and char-forming capability of MoB_2, which helps dissipate energy effectively while maintaining structural integrity. In contrast, the pure alumina coating, despite its low reflectivity, resulted in a higher backside temperature—likely due to its higher thermal conductivity and direct energy transfer. Overall, the $Al + MoB_2$ composite offers a favorable combination of reflectance control,

	thermal insulation, and durability, positioning it as a strong candidate for protective coatings against HEL threats in defense and aerospace applications.
22.	Abrupt autofocusing and scintillation dynamics of truncated circular airy derivative beams in strong turbulence **A Kumari, V Pal** - Optics Communications, 2026 **Abstract:** We present a combined experimental and numerical study on the abrupt autofocusing and scintillation dynamics of truncated circular Airy derivative beams (CADBs) in free space and in strong turbulence. Inner and outer truncations of up to 60% are applied to investigate the impact of structural modifications on beam propagation. The autofocusing strength, quantified by the maximum K-value, is found to decrease systematically with increasing truncation. Inner truncation maintains higher maximum K-value but demonstrated increased sensitivity to turbulence. In contrast, outer truncation yields lower maximum K-value while offering enhanced robustness under turbulent conditions. Despite strong turbulence, all truncated CADBs exhibit a notable rise in their K-value, confirming the resilience of their intrinsic self-accelerating autofocusing behaviour. Further, scintillation index analysis reveal that self-healing governs turbulence response: inner truncation delays but intensifies scintillation due to core reconstruction, whereas outer truncation allows faster stabilization with reduced fluctuations. These results highlight truncation as a tunable parameter for balancing focusing strength and turbulence robustness, with relevance to free-space optical communication, imaging, and optical trapping.
23.	Achieving high tensile strength and ductility in refractory alloys by tuning electronic structure H Huang… **D Beniwal, PK Ray**…N Argibay - Nature Materials, 2026 **Abstract:** he energy efficiency of heat engines (gas and steam turbines) for electricity production and propulsion is determined by the Carnot cycle and scales with operating temperature. Commercial nickel- and cobalt-based superalloys melt near 1,500 °C and rapidly lose mechanical strength beyond 1,000 °C. Refractory metals melt well above 2,000 °C but have inherent manufacturability challenges that are barriers to adoption, such as high ductile-to-brittle transition temperatures. Using density functional theory-guided design, we demonstrate tailored local lattice distortions that promote phase-stable, non-equiatomic refractory concentrated solid solutions with both high ductility and strength. We exemplify this for single-phase, body-centred cubic $Nb_4Ta_4V_3Ti$ that exhibits castability, excellent room-temperature tensile yield strength (~1 GPa) and ductility (approaching 20% uniform strain), and exceptional high-temperature tensile strength (500 MPa at 1,000 °C). These findings illustrate a path for designing materials that hold great potential for advancing next-generation technologies such as Generation IV fission reactors, first-generation fusion-plasma reactors, and more efficient gas turbines for electricity generation and propulsion.
24.	Admission control and pricing for multi-tenant network slices in 5G: A learning perspective **S Dhamal,** W Ben-Ameur, T Chahed - Computer Networks, 2025 **Abstract:** Network slicing is a critical component in 5G, where each slice can be customized for a given type of service, and a given tenant characterized by a stochastic demand and a resource utility function reflecting its Quality of Service requirements. Considering the slice market as a Stackelberg game, the operator, as the leader, presents pricing for each demand interval and slice type, and the tenants, as followers, decide which demand interval to request. The operator jointly determines the pricing and admission that maximize its revenue while satisfying its capacity constraint. We show NP-hardness of this problem, and a paradox that the operator's revenue could decrease if a tenant's resource utility increases. We consider a practical scenario where the tenants' resource utilities are not known to the operator. For learning an optimal pricing, we propose online approaches based on iteratively updating the operator's knowledge regarding the resource utilities

	post its interactions with the tenants, and an offline approach based on neural networks. We study these with respect to various metrics: achieved revenue, reliability, and learning rate. One of our approaches consistently achieves near-optimal revenue irrespective of the number of tenants, with over 95% of optimal revenue within 20 interactions on average.
25.	Advancing nanobubble-assisted crystallization as a green and sustainable technology **A Sharma, T Kaur, N Nirmalkar** - ACS Sustainable Chemistry & Engineering, 2026 **Abstract:** Crystallization is a key process in the chemical industry for manufacturing, separation, and purification. However, precise control over the crystal properties remains challenging. Ultrasound-assisted crystallization has been widely used to overcome these issues, but its continuous use can cause thermal degradation, reactor corrosion, and high energy consumption, limiting industrial scalability. Nanobubbles offer a green, sustainable alternative due to their high surface-to-volume ratio and strong negative surface charge, which promote nucleation and control crystal growth. This study compares ultrasound and nanobubbles in cooling crystallization. A theoretical analysis using a modified Gibbs free-energy equation showed that increased nanobubble surface charge reduces nucleation energy barriers by providing a relation of … Experimentally, nanobubbles shortened induction times, increased yield, and reduced crystal size from 171 to 83 μm. The variation in operating parameters for nanobubble production resulted in optimum conditions for crystallization. Overall, nanobubbles present a viable, non-invasive alternative to ultrasound, offering effective crystallization control without significant energy input, making them suitable for industrial-scale applications. 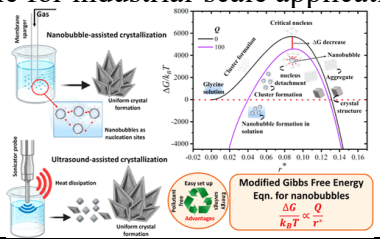
26.	Analytical study of orthotropic inhomogeneous beams under transverse loading: A. Amandeep, SS Padhee **Amandeep, SS Padhee** -Archive of Applied Mechanics, 2026 **Abstract:** This work presents the application of variational principles to an inhomogeneous beam having orthotropic material properties. A planar beam with arbitrary transverse loading has been considered. Variational asymptotic method (VAM), a synergy between variational principles and asymptotic expansion, has been used. Application of VAM has simplified the analysis by assisting in providing the solution equations in an ordinary differential equation (ODE) format. Moreover, these equations are in functional form. ODEs are easier to solve and facilitate a closed-form analytical solution, whereas the functional form widens the scope of these equations by permitting solutions for a wider class of inhomogeneity models. For illustrations, four different inhomogeneity models are adopted from the literature, and a closed-form solution for each has been presented. The verification of the obtained results has been done by comparing them with some of the prominent literature results, as well as with finite element analysis (FEA) results obtained using Abaqus. Furthermore, it has been observed that the analytical solutions of this study also perform very well in situations involving isotropic material properties. There has been a considerable savings in computational cost between an FEA analysis and the analytical analysis. Based on this, the following are some of the key contributions from this work: (a) The given formulation successfully handles orthotropic as well as isotropic materials. Isotropy is handled by doing suitable reductions in the stiffness coefficients of the orthotropic material matrix. (b) In line with the mechanics, the ordered warping solutions result in Euler–Bernoulli-type deformation in the zeroth order, whereas the higher-order solutions result in transverse shear contribution.

27.	Arsenate adsorption onto hydrous ferric oxide: Insights from triple layer surface complexation modeling **H Nazir, R Moozhikkal, B Thakur, S Pathak, PP Singh** - Journal of Geochemical Exploration, 2026 **Abstract:** This study investigates arsenate [As(V)] adsorption dynamics along soil depth profiles in natural soils from Gurukhwind village, Tarn Taran district, Punjab, using batch adsorption experiments in an arsenic (As) affected region. Kinetic experiments showed rapid As(V) adsorption within the first 4 h, reaching equilibrium at 12 h across all soil layers. As(V) adsorption was substantially higher in surface soil layers than in bottom layers, largely due to variations in surface area, organic matter content, pH, and mineralogical components such as hydrous ferric oxide (HFO). Adsorption decreased with increasing pH, with maximum uptake occurring under acidic conditions due to enhanced electrostatic forces of attraction between protonated surface sites and negatively charged As(V) species. The pseudo-first-order (PFO) model best described the kinetic data, while equilibrium data followed the Langmuir isotherm, indicating monolayer adsorption, with R^2 values exceeding 0.9 across all soil layers. The 2-pK Triple Layer Model (TLM) successfully simulated the pH-edge and isotherm trends for As(V) adsorption on HFO, suggesting the formation of dominant inner-sphere complexes = $Fe(H_2AsO_4)$, =$Fe(HAsO_4)^-$ and = $Fe(AsO_4)^{2-}$ along with minor contribution from outer-sphere complexes $FeOH_2^+$_ $H_2AsO_4^-$ and $FeOH_2^+$ _ $HAsO_4^{2-}$. The good agreement between modeled and experimental data was supported by reasonable RMSE values for isotherms and pH-edge data. The combined findings underscore the importance of iron (Fe) oxide rich surface horizons in controlling As mobility, with direct implications for the development of site specific management and mitigation strategies in As affected regions.
28.	Arsenic release dynamics in Punjab's agricultural soils: The role of background species using fractional factorial design **H Nazir, M Raheena, B Thakur, PP Singh** - Discover Soil, 2026 **Abstract:** Arsenic contamination has become an important environmental issue in India, particularly in Punjab, where intensive agriculture and groundwater dependence have exacerbated the problem. However, limited attention has been paid to the effects of arsenic release from soils and the role of background species in this process. This work investigates arsenic (As) release from agricultural soils at different depths in Theh Kalan village, Tarn Taran district, Punjab, and examines the effects of background species using batch experiments. Arsenic release followed the order: subsoil > bottom soil > topsoil, with higher release in the absence of background species. The impact of six ionic species (SiO_3^{2-}, PO_4^{3-}, HCO_3^-, SO_4^{2-}, Ca^{2+}, and Cl^-) was assessed using a 2^{6-2} fractional factorial design (FFD). In single-ion systems, PO_4^{3-}, SiO_3^{2-}, and HCO_3^- increased release, SO_4^{2-} and Cl^- had slight effects, while Ca^{2+} reduced release. In multi-ion systems, $PO_4^{3-} > SiO_3^{2-} > HCO_3^- > SO_4^{2-}$ enhanced release, whereas $Ca^{2+} > Cl^-$ limited it. Significant interactions of $SiO_3^{2-} \times PO_4^{3-}$ and $SiO_3^{2-} \times HCO_3^-$ were observed. Model adequacy was evaluated using ANOVA and residual analysis. These findings highlight the strong influence of background species on arsenic release from soils and their implications for groundwater contamination.
29.	Assessment and analysis of hardness for bobbin tool-friction stir welded joint for aa 6063 using Taguchi technique and abaqus software S Kumar, M Maurya, **S Bansal,** Aniruddha- Physics of Metals and Metallography, 2025 **Abstract:** Nowadays, aluminum alloys can be safely welded by using bobbin tool friction stir welding (BT-FSW) having various advantages over the fusion welding process. This research work was carried out to evaluate the welding process parameters such as tool rotation speed, tool pin diameter and welding speed affecting the mechanical performances of welded AA 6063 sheets.

	Taguchi technique was used to analyse the influence of process parameters on the hardness of the welded joint. L_9 orthogonal array and the analysis of variance was employed to investigate the importance of process parameters for their responses. Experimental results revealed that the hardness of the welded joint was improved with increasing the tool rotational speed and tool pin diameter. The hardness was decreased with increasing the welding speed. The analysed results were verified in the confirmation experiments. The optimal hardness value 92 HV was achieved for the welded joint at the 1200 rpm tool rotation speed, 5.5 mm tool pin diameter, and 50 mm/min welding speed. The FSW process was simulated using Abaqus software to compare the results. The microstructure analysis for different zones of the weld joint and scanning electron microscopy for the welded joint was also performed.
30.	Biodegradable cellulosic aerogels for rapid and efficient adsorptive removal of ciprofloxacin and methylene blue from contaminated water **R Ranjan,** M Kullappan, **SP Gumfekar, M Sabapathy** - Journal of Hazardous Materials Advances, 2026 **Abstract:** Once celebrated as milestones of scientific progress, activated pharmaceutical ingredients (APIs) now fuel a growing crisis — their unchecked release into aquatic environments accelerates antimicrobial resistance, endangering human and animal health globally. Conventional remediation strategies often suffer from inefficiency, high operational costs, and limited scalability. Here, we demonstrate cellulosic aerogels, synthesized via a sol–gel process and subsequent lyophilization, as sustainable bio-adsorbents for removing ciprofloxacin (CIP), an API, and methylene blue (MB) from contaminated water. Structural characterization via FESEM and BET analysis confirmed a hierarchical porous network with a specific surface area of ≈ 398 m^2/g and large pore volume. Batch adsorption experiments demonstrated highest affinity for CIP and MB, achieving maximum adsorption capacities. The adsorption processes followed pseudo-second-order kinetics with a good correlation coefficient. Mechanistic investigation revealed that adsorption is predominantly governed by strong π-π stacking interactions between the aromatic structures of ciprofloxacin and the cellulose matrix, supplemented by hydrogen bonding and electrostatic attractions. Additionally, zeta potential measurements indicated a negatively charged surface (-25 ± 2 mV), enhancing interaction with cationic pollutants. Our findings highlight the potential of biodegradable cellulosic aerogels as efficient, low-cost alternatives to synthetic adsorbents, offering a scalable solution for antibiotic removal and broader applications in wastewater treatment technologies. 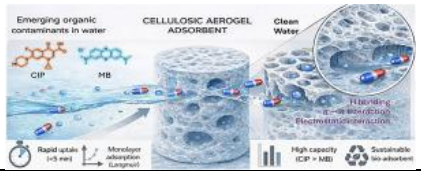
31.	Chaotic advection in regional groundwater flow under periodic water table fluctuations: An analytical model with depth-dependent aquifer properties **S Maurya, R Sarmah, I Sonkar** - Advances in Water Resources, 2026 **Abstract:** Reliable prediction of groundwater flow dynamics is often hindered by the assumption of uniform aquifer parameters, leading to biased estimates of hydraulic head. Despite their well-established depth-dependence relationship, most analytical solutions remain restricted to homogeneous or single-layer aquifer systems. This study develops a two-dimensional transient analytical model for a multilayer regional aquifer driven by a fluctuating water table, explicitly incorporating depth-dependent hydraulic conductivity and specific storage while accounting for pumping. The analytical solution is derived using the Generalized Integral Transform Technique (GITT), ensuring implicit continuity of head and flux across layer interfaces without requiring

	iterative eigenvalue estimation, providing a rigorous framework to capture the complexities of stratified aquifers. Model verification is performed against a benchmark single-layer solution, and independent validation is carried out with COMSOL Multiphysics simulations, showing excellent agreement. Parameter influence and reliability are further assessed through global sensitivity analysis and uncertainty evaluation. A novel contribution of this work is the identification of chaotic flow behaviour within a three-layer Tóthian basin, analyzed using the Finite-Time Lyapunov Exponent (FTLE). Results show that chaotic dynamics are most pronounced near the upper boundary, where FTLE values are significantly higher than in deeper zones and further enhancement is observed under periodic injection. Moreover, specific storage is found to enhance the swirly motion of particle trajectories, increasing residence times near pseudo-stagnation zones. The proposed analytical framework bridges a critical gap in multilayer transient flow modeling, advances the theoretical understanding of stratified aquifer systems, and provides a robust benchmark for numerical and field-scale groundwater investigations. 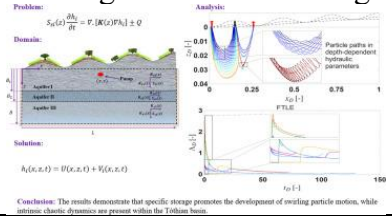
32.	Charged black hole with string cloud deformation: Entanglement and chaos S Pant, S Kaushal, **A Maurya,** H Parihar - Physical Review D, 2025 **Abstract:** We perform a holographic analysis of several quantum information-theoretic observables—entanglement entropy (EE), mutual information (MI), entanglement wedge cross section (EWCS), butterfly velocity (vB), and thermo mutual information (TMI)—in the background of charged anti–de Sitter (AdS) black hole deformed by a homogeneous string cloud. This configuration is dual to a large $\mathcal{N}c$ strongly coupled field theory at finite temperature and finite chemical potential, in presence of quark-cloud. We study how the entanglement structure and chaotic dynamics in the boundary theory are affected by the charge and backreaction. In our observation we find that both EE and EWCS increase monotonically with charge and backreaction, indicating enhanced correlations due to additional degrees of freedom. On the other hand MI and TMI show a more intricate dependence: backreaction tends to strengthen correlations, while increasing charge suppresses entanglement and makes the system more susceptible to scrambling. The analysis of the butterfly velocity vB indicates that the presence of charge and the backreaction suppress the chaotic behavior of the system by. Furthermore, TMI exhibits a sharp transition under shockwave perturbations, with interboundary entanglement being entirely disrupted beyond a critical shock strength, which decreases with increasing charge.
33.	Coarse slip bands and non-Schmid's translational slip lead to shear bands formation in body-centered cubic HfNbTaTiZr high-entropy alloy LK Singh, **A Lavakumar,** RR Eleti - Scientific Reports, 2025 **Abstract**: The microstructural evolution and shear band formation mechanism in an equiatomic HfNbTaTiZr body-centered cubic (BCC) high-entropy alloy (HEA) were systematically investigated during cold rolling. Microstructural observations revealed the development of coarse, and straight slip bands at early deformation stages. Detailed analysis of slip band–grain boundary (GB) interactions showed evidence of continuous slip transmission across GB regions. With increasing deformation, localized strain regions evolved along the prior slip bands, eventually leading to the formation of well-defined shear bands. Non-Schmid effects were found to promote slip continuity across GBs, preferentially along the {112} slip planes, thereby facilitating strain localization. The present study highlights the critical role of flow localization on {112} planes,

	non-Schmid deformation behavior, and strain accommodation mechanisms particularly at slip band–GB intersection regions in governing shear band formation in the HfNbTaTiZr BCC-HEA.
34.	Cooperative effect of oxygen vacancies and lewis acid sites in selective depolymerization of PET plastic over Ti-doped ZnO catalysts **R Das, AK Manal, R Srivastava** - ChemCatChem, 2026 **Abstract:** Effective and selective recycling of polyethylene terephthalate (PET) into monomers and chemicals is essential. Herein, transition metal-doped ZnO catalysts (M = Ti, Zr, and Hf) were synthesized and investigated for PET methanolysis. Among them, the Ti-doped ZnO catalyst containing 7.5 wt% Ti (7.5Ti–ZnO) exhibited excellent activity, delivering 98.3% dimethyl terephthalate (DMT) yield at 170°C in 0.5 h, representing a 2.5-fold higher activity than pristine ZnO. The catalyst also showed excellent activity in real and mixed PET wastes, confirming its broad applicability. Structural and spectroscopic analyses confirmed the incorporation of Ti into the ZnO lattice, resulting in a homogeneous solid solution with lattice distortion and an abundance of oxygen vacancies. NH_3–TPD measurements revealed a substantial increase in acid sites with optimal Ti loading (7.5 wt%). The cooperative effect between oxygen vacancies and medium-strength Lewis acid sites facilitated PET and methanol activation, and subsequent C–O dissociation via nucleophilic attack by methanol. Consequently, 7.5Ti–ZnO achieved a remarkable DMT formation rate of 510 $mmol_{DMT}\ g_{cat}^{-1}\ h^{-1}$. This study further underscores the potential of DMT as a versatile feedstock for the synthesis of virgin-quality PET and other high-value monomers, thereby enabling both closed-loop recycling and open-loop upcycling pathways toward a circular plastic economy. 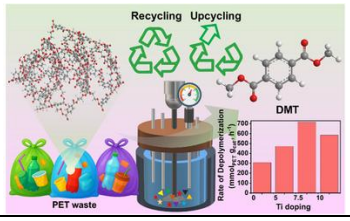
35.	Data driven deep neural network based task offloading on edge cloud continuum **M Sahi, N Auluck,** A Azim, **P Bhardwaj,** MA Maruf - IEEE Transactions on Network and Service Management, 2025 **Abstract:** Edge computing reduces bandwidth bottlenecks and latency by performing computations close to end-users, making it a viable option for application task offloading. Owing to its limited computational capacity, the cloud may need to be considered with the edge for offloading. Task offloading is challenging, because of the availability of limited resources, dynamically changing network conditions, and concurrent user access. Mathematical task offloading approaches may be incapable of capturing dynamic network situations in large end-to-end network models. We propose D2-TONE (Data-driven Deep Neural Network Task Offloading on the Network Edge), an approach that employs Machine Learning (ML) algorithms to accurately estimate offloading costs, such as computation and transmission costs. D2-TONE adapts holistically to dynamic network situations, and provides optimal/near-optimal offloading solutions in real-time. In addition, D2-TONE employs the distributed execution of Deep Neural Network (DNN) training tasks on the edge-cloud continuum. Experiments revealed that D2-TONE reduces the training time by 1.55 to 2.77 times, compared to baseline approaches. In addition, the edge based D2-TONE offers an improvement of 55-76% in the data processing ratio, compared to other offloading approaches.
36.	Developing sustainable and resilient supply chain: Industry 4.0 drivers, dynamic capabilities, and performance evaluation **C Dixit, R Kumar,** A Kumar - Production Planning & Control, 2026

	Abstract: Industry 4.0 technologies have emerged as a critical strategic resource for firms seeking to enhance supply chain capabilities and improve both economic and environmental performance. However, the mechanisms through which these technologies translate into superior supply chain performance remain insufficiently understood. To address this gap, grounded in organisational information processing theory (OIPT), this study examines the impact of Industry 4.0 technologies on dynamic capabilities and the subsequent influence of capabilities on supply chain performance. The study draws on primary data collected from firms operating in multiple industrial sectors, including automobiles, electronics, textiles, and pharmaceuticals, and employs partial least squares structural equation modelling to test the hypotheses derived from the conceptual framework. The results demonstrate that Industry 4.0 enabling technologies enhance core supply chain dynamic capabilities, including visibility, resilience, and sustainability. Furthermore, supply chain visibility plays a crucial role in positively influencing supply chain resilience and partially mediating the relationship between Industry 4.0 technologies and supply chain resilience. Overall, this study advances understanding of how Industry 4.0 technologies translate into superior supply chain capabilities and performance, offering actionable insights for supply chain managers and policymakers on designing and integrating digitally enabled supply chains.
37.	Designing future ornamental plants: An integrated roadmap for precision biotechnology **DA Mosoh,** WA Vendrame - Frontiers in Horticulture, 2026 **Abstract:** The global floriculture industry, a multi-billion-dollar enterprise driven by consumer demand for novelty and confronting urgent pressures for greater sustainability, is at a transformative inflection point. While conventional breeding has been successful, it is often slow and constrained by the genetic limitations of sexual compatibility and the inherent biology of target species. The advent of precise genome editing (GE) technologies, particularly the CRISPR-Cas system, offers an unprecedented opportunity to accelerate ornamental improvement. This literature-based review examines the immense potential of an expanded genomic toolbox—including base, prime, and epigenetic editing, as well as synthetic biology— to rationally design complex traits such as vibrant color, enhanced fragrance, extended vase life, and stress resilience. However, a significant "transfer gap" persists between major agronomic crops and ornamental species. The path from laboratory innovation to commercial reality is impeded by formidable challenges: many elite cultivars possess highly heterozygous and polyploid genomes, which complicates gene targeting, while a widespread dependency on recalcitrant, genotype-specific tissue culture systems creates a critical bottleneck for transformation. Here, a critical analysis is presented regarding these biological hurdles and the equally complex non-technical maze of intellectual property, fragmented global regulations, and public perception. It is argued that ornamental plants, as non-food crops, represent an ideal platform for pioneering rational, product-based regulatory frameworks and fostering societal acceptance. The article concludes with a call for a new, interdisciplinary paradigm that unites plant scientists with engineers, computational biologists, and social scientists. This integrated roadmap, focused on building a comprehensive "genome-to-phenome" data ecosystem and redefining the value of ornamentals beyond aesthetics to include tangible ecosystem services, is essential to co-create a scientifically sound and socially robust future for ornamental biotechnology.
38.	EcoSense: An autonomous polarization-insensitive wireless-powered battery-free IoT beacon for live environmental sensing **VK Malav, A Sharma** - IEEE Transactions on Instrumentation and Measurement, 2026 **Abstract:** The battery-free wireless sensor beacons (WSB) are essential for realizing a green and self-sustainable operation for power-constrained Internet of Things (IoT) applications. With increasing communication activities and availability, the radio frequency (RF) energy harvesting

	(EH) using a rectenna has become a reliable solution to energize the WSB wirelessly. Prior literary works indicate that the EH of a rectenna depends on the wave polarization between the rectenna and the transmitter to effectively capture the maximum incoming waves from any orientation, allowing the deployment of IoT nodes without requiring specific alignment. However, simultaneous effective EH and data transfer over a long distance at ultralow power is still an issue. Therefore, a novel RF-powered battery-free IoT beacon with a polarization-insensitive (PoI) feature is developed and demonstrated for ultralow-power IoT sensing applications. This WSB is completely integrated and miniaturized by implementing both wireless power and data transfer, which is developed on a multilayer printed circuit board (PCB). The WSB consists of a rectenna array operating at 5.2 GHz for wireless power, an integrated circuitry of a power management unit (PMU), and a Bluetooth low energy (BLE) module for data transfer. The WSB operates at a minimum received microwave power of −15.18 dBm. The results demonstrate the system to be wirelessly energized at a transfer range of 11 m away from the transmitter emitting 47.22 dBm power and realizing battery-free operation for IoT sensors. Thus, this design is suitable for orientation-independent WSB operations in IoT applications such as environmental monitoring and smart agriculture applications in remote areas.
39.	Effect of curing conditions on the physical, chemical, and dielectric properties of AC XLPE insulation **SM Anas, CC Reddy** - IEEE Transactions on Dielectrics and Electrical Insulation, 202 **Abstract:** This research investigates the effect of curing conditions on the structural, chemical, and electrical properties of AC cross-linked polyethylene (XLPE). XLPE sheet specimens are prepared in our lab by curing at different temperatures (150–300°C) and for different durations (10–120min) in order to examine their impact on material performance. The specimens are further subjected to Fourier Transform Infrared Spectroscopy (FTIR), X-ray Diffraction (XRD), Differential Scanning Calorimetry (DSC), Scanning electron microscopy (SEM) and the degree of cross-linking tests for material characterization, whereas AC conductivity measurements, dielectric loss tangent (tan δ) tests and breakdown tests are performed for electrical characterization. The results are analyzed extensively and an intricate relationship is observed between the effect of cross-linking, degree of crystallization, carbonyl index and AC breakdown strength. The findings are believed to be useful for AC cable manufacturers and utilities.
40.	Electrokinetic and electro-elastic instabilities in viscoelastic microfluidic flows: Suppression and augmentation in mixing efficiency **C Sasmal, T Waghmare, A Chauhan** - Soft Matter, 2026 **Abstract:** Viscoelastic fluids, such as polymer solutions, surfactant mixtures, colloidal suspensions, emulsions, and biological fluids like blood, are frequently transported in microfluidic systems using external electric fields. In such flows, two distinct types of instabilities can emerge, namely, electro-elastic instabilities (EEI), arising from the interaction between elastic stresses and streamline curvature, and electrokinetic instabilities (EKI), triggered by electrical conductivity gradients once the external electric field exceeds a critical value. Both instabilities can promote fluid mixing by inducing chaotic flow structures; however, their roles are not always complementary. Recent experimental and numerical studies have shown that increasing fluid viscoelasticity can suppress EKI, leading to reduced mixing efficiency in a microfluidic T-junction. However, this study demonstrates that while viscoelasticity initially hinders mixing by damping EKI, a further increase in the Weissenberg number (a measure of fluid elasticity) leads to the onset of EEI, which in turn again increases mixing. Therefore, a non-monotonic relationship between mixing efficiency and Weissenberg number is found in the present study. Furthermore, although both EEI and EKI promote mixing, they differ significantly in their coherent flow structures and regions of origin within the microdevice. To elucidate these differences, we employ

	the data-driven dynamic mode decomposition (DMD) technique to characterise the underlying instability modes and their influence on the mixing dynamics. Overall, this study provides fundamental insights into how viscoelasticity modulates flow instabilities in electrokinetically driven microflows and offers strategies to optimise mixing by tuning fluid properties and operating conditions.
41.	EMI shielding performance of commercial aluminium foil and Cu-Ni conductive fabric A Singh, **GP Singh, N Sardana** - Journal of Physics: Conference Series, 2025 **Abstract:** Shielding devices from electromagnetic waves is important for effective functioning and security. Metals possess very good shielding properties due to their high conductivity. The current article investigates the factors influencing the shielding efficiency of on aluminium sheet/foil and copper nickel (Cu-Ni) conductive fabric. The conductivity, thickness, and amount of preformation influences the efficiency of aluminium and Cu-Ni conductive fabric in mitigating electromagnetic interference (EMI). The experimental data gathered from measuring shielding effectiveness across a spectrum of frequencies (1-18 GHz) were studied to understand the influence of these factors on the overall performance of shielding. The findings from this research enhance our comprehension of the factors impacting EMI shielding efficiency, guiding the development and enhancement of shielding solutions for various electronic applications.
42.	Energy-efficient gas sensing of NO and NO_2 at room temperature using poly(triarylamine) organic semiconductor A Chaurasiya, **AK Singh,** D Panda - IEEE Sensors Journal, 2025 **Abstract:** Nitrogen dioxide (NO2) and nitric oxide (NO) are among the most hazardous environmental gases, primarily generated from fossil fuel combustion, and power plants, posing a serious challenge for achieving sustainable development goals (SDG 3). Poly(triarylamine) (PTAA), a polymer with a delocalized -conjugated backbone has been investigated for its efficacy in gas sensing under ambient conditions. Herein, a PTAA thin-film semiconductor gas sensor is fabricated and systematically evaluated for the detection of NO2 and NO at room temperature. Thin films of PTAA are deposited onto prefabricated interdigitated electrodes (IDEs) by drop-drying a solution of PTAA in chloroform, ensuring straightforward device integration. The structural and morphological features of PTAA are characterized by using spectro-microscopic techniques. The fabricated sensors exhibit clear and reproducible responses of 70.8% and 27.8% toward 5 ppm NO2 and NO, respectively, supported by repeatability, response, and recovery characteristics. In addition, the PTAA sensor showed the highest NO2 selectivity when tested against common exhaust pollutants (H2S, SO2, and NH3). The response and recovery times toward NO2 were recorded as 295 and 505 s, respectively, highlighting superior sensitivity and faster recovery dynamics when compared to NO. These findings establish PTAA as a promising organic semiconductor for the selective detection of NOx gases. 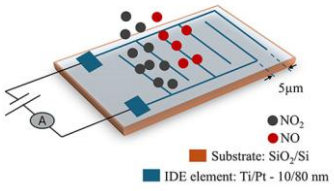
43.	Enhanced selectivity by planar hyper-coordinate transition metals for biosensing Z Zhang, **R Ahuja,** W Luo - Advanced Theory and Simulations, 2026 **Abstract:** Selectivity in sensitive biosensing requires avoiding multi-enzyme-like activity, but suppressing the multi-enzyme-like activity of transition metals remains challenging. Recently, planar hyper-coordinate states have led to an emerging family of 2D materials with strong planar

	confinement. Here, we propose a possible strategy to enhance the selectivity of biosensing using planar hyper-coordinate transition metals, and verified our strategy through simulations of the planar hyper-coordinate 2D materials $ScCN_3B_6$ and the non-planar 2D material YCN_3B_6 for the adsorption of biomolecules, including adenosine, ascorbic acid, and nucleobases. Breaking the planar confinement of $ScCN_3B_6$ leads to enhanced adsorption of analytes. In contrast, YCN_3B_6 does not show selectivity in the same systems compared with $ScCN_3B_6$. Therefore, whether the planar confinement is broken provides a possible route to enhance selectivity. Moreover, the arrangement and synergy of transition metal active sites improve the adsorption energy to specific molecular structures. The development of planar hyper-coordinate transition metals opens a fertile playground for highly selective label-free biosensing.
44.	Enhancing cold-sprayed nickel–aluminum bronze coatings on magnesium via scanner-based laser remelting **G Vinay, R Kant,** A Piiroinen, C Nayak, A Ganvir, **H Singh** - Journal of Thermal Spray Technology, 2026 **Abstract:** Nickel–aluminum bronze (NAB) coatings are widely used in marine and industrial applications due to their excellent corrosion resistance, but their deposition on soft, low-melting substrates such as magnesium (Mg) remains challenging. This study investigates the cold spray deposition of as-received and heat-treated NAB (unsegregated) powders on Mg and NAB substrates, followed by post-processing using a fine-beam scanner-based laser remelting system. The as-deposited coatings improved the corrosion resistance of Mg substrates; however, they exhibited high porosity ($5.2 \pm 0.7\%$) and poor inter-splat bonding, as evidenced by the dislodgement of weakly bonded splats during polishing. Laser remelting with optimized parameters selectively fused layers to depths ranging from ~ 42 μm to ~ 220 μm. By remelting only the top surface layers (~63 μm), surface porosity, and inter-splat defects were sealed effectively, while the underlying cold-sprayed microstructure remained unaltered. Phase analysis confirmed martensitic transformation in the remelted layer, with no detectable oxidation due to effective argon shielding. Electrochemical testing revealed a 52% reduction in corrosion current density after remelting. This study demonstrates the feasibility of utilizing scanner-based laser remelting as a post-processing method, offering a controllable approach for selectively refining cold-sprayed coatings made of hard and brittle materials on soft substrates.
45.	Experimental demonstration of enhanced displacement by phase separation in a two-dimensional milli-model in viscously unstable fluid displacement S Kiuchi, Y Nagatsu, T Ban, **M Mishra,** RX Suzuki - Physical Chemistry Chemical Physics, 2026 **Abstract:** Interfacial phase separation in flowing systems has emerged as a key phenomenon in soft matter and interfacial science, particularly because of its coupling with interfacial hydrodynamics. Although viscous fingering (VF) has been widely explored in fully miscible and immiscible systems in porous media or Hele-Shaw cells, the pore-scale dynamics of partially miscible systems undergoing phase separation inside porous structures remain virtually unknown, despite their direct relevance to multiphase transport and enhanced displacement in geological and industrial processes. Herein, we present the first experimental demonstration of partially miscible VF in a porous-media-like two-dimensional milli-model, which explicitly incorporates pore and throat geometries. By systematically comparing fully miscible, immiscible, and partially miscible systems, we reveal that partially miscible displacement generates pore-scale droplet formation, self-propelled droplets, pore-geometry-dependent droplet bypassing and splitting, the interaction between self-propelled droplets and pore throats, and channel redirection and spreading induced by droplet-generated resistance. Quantitative analysis using several indicators—interfacial tension difference, droplet number, area density, and angular fluctuation amplitude—shows that the displacement efficiency increases monotonically with the magnitude of phase separation. We

	consider that this increase is due to the cooperative action of Korteweg-force-driven convection and droplet-induced Jamin blocking. Our finding of enhanced spreading is unique to partially miscible flows in porous structures and demonstrates how thermodynamic instability can be harnessed to control and improve displacement processes.
46.	Fission fragment distributions of the excited compound nucleus in $^{14}N+^{175}Lu$ reactions at energies below 7 MeV/A SK Gautam… **PP Singh**…R Prasad - The European Physical Journal A, 2026 **Abstract:** The present study focuses on the measurement and analysis of the cross sections of 35 fission like residues (with mass numbers $74 \leq A \leq 111$) and 10 fusion-like residues in the 14N+175Lu reactions at energies ≈ 75.8MeV, 79.7 MeV and 84.0 MeV, respectively. The measurements have been carried out using the recoil catcher technique followed by off-beam activation γ -ray spectroscopy. Analysis of fusion reaction data reveals the presence of complete and incomplete fusionmechanisms in the 14N+175Lu reactions at these energies. In addition to the fusion contribution, a substantial amount of fission following the complete and incomplete fusion is also observed. The experimentally deduced post-fission observables mass (σA) and charge (σZ) dispersion parameters from the isotopic and isobaric distributions of fission fragments are found to be in good agreement with their values reported in the literature and calculated theoretically as well. Such consistency refers to the production of these fission fragments from the equilibrated compound nucleus (189 $Pt*$) in 14N+175Lu reactions. This finding is also verified by the observations of the symmetric mass distributions of fission fragments which are found to have a singlehumped Gaussian shape and theirmass variances ($\sigma 2M$) follow the exponential trend with excitation energy, a characteristic of compound nucleus fission. The consistency in the isotopic, isobaric and mass distributions of the fission fragments in the 14N+175Lu system enhances an additional understanding of compound nucleus fission in heavy-ion reactions.
47.	Flexible MoS2-based ion-selective sensor with valinomycin membrane for in-situ detection of soil potassium (K) ions **P Shukla, R Gond, B Rawat** - IEEE Sensors Letters, 2026 **Abstract:** In this letter, we report the flexible MoS2/valinomycin-based sensor for in situ K+ detection in the soil sample. The fabricated sensor, realized on a flexible PET substrate using scalable ink-dispensing techniques, exhibits a wide detection range of 1–100 mM with high linearity (R2 = 0.9975) and sensitivities of 5.6 µA/mM in analyte solution and 2.1 µA/mM in soil sample. More importantly, cyclic voltammetry analysis reveals stable and reversible oxidation–reduction behavior across repeated cycles, with excellent reproducibility in multiple sensor replicas. The fabricated sensor uniquely combines soil compatibility, flexibility, reproducibility, and cost-effective fabrication, which addresses the critical gap between laboratory sensing technologies and field-deployable soil nutrient monitoring. These results establish the MoS2/valinomycin sensor as a robust and scalable platform for precision agriculture, with the potential to advance real-time nutrient management and promote sustainable farming practices. 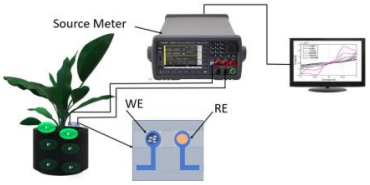
48.	"… Grey and Cold and Full of Long Shadows": City, neoliberalism and alienation in the 1970–80s American horror literature **A Das, D Ray** - Humanities and Social Sciences Communications, 2025

	Abstract: This paper investigates American urban horror novels from the 1970s to 80s with a specific focus on the theme of alienation. While analysing the specific theme, the paper tracks the nuanced manifestations of neoliberalism-induced greed and exploitation and brings forward a portrait of the evolving urban landscape. Based on the treatment of urban themes in the selected texts, we have divided the paper into two sections: the redemptive arc of the 70s and the city-beyond-redemption in the 80s. The first section–focused on the exploitation of the socio-economic minority by the urban upper class–talks about a 'hopeful' climax of resistance. The second section concentrates on the 'city-beyond-redemption': a hopeless, dystopic and indifferent space in the grip of neoliberal greed and deprivation that drives the citizens into a self-destructive impulse. Our paper tracks this thematic evolution through a wide spectrum of canonical American horror literature, from classics by Ira Levin, William Peter Blatty and Jay to the 'Splatterpunk' and Cosmic Horror/New Weird genre popularised by John Skipp, Craig Spector and Kathe Koja, etc. We argue that the city-themed American horror literature of the 1970–80s reflects a detailed and variegated impact of the neoliberal era on American society, acting as an important marker of the evolution of urbanity, social struggle and human existence in general.
49.	Gradient-based compression and approximate computing for deep network optimization in multimedia data processing VK Singh, **J Singh,** RS Rathore, D Nema - IEEE Transactions on Consumer Electronics, 2026 **Abstract:** Existing methods of compressed multimedia data processing in deep networks are constrained by inherent trade-offs such as low reconstruction accuracy, compression ratio, and high computational latency. With computational intensive tasks, the performance further deteriorates owing to high energy requirements and processing delays in real-time, large-scale multimedia applications. This work presents a deep learning framework that integrates gradient-based compression with approximate computing to optimize the in-network processing of multimedia data. Hyperparameter tuning is employed to systematically adjust bit-width, model size, and network depth, enabling fine-grained control over compression and computational efficiency. The proposed approach makes use of adaptive convolutional layers and dynamic learning rates for local gradient residue compression with the aim to improve the exploitation of low-rank structures and data sparsity. Extensive simulations are performed on publicly available datasets, including CIFAR-10, CIFAR-100, and MNIST, to validated the performance of the proposed method. Results demonstrate the effectiveness of the proposed method as it outperforms a set of state-of-the-art approaches achieving a classification accuracy of 99.09%, with almost real-time processing of the multimedia data.
50.	GreenEdge AI: Sustainable federated learning for smart city air quality prediction **S Dey,** R Raina, **S Mishra**… R Dharavath - Journal of Industrial Information Integration, 2026 **Abstract:** Rapid urbanization and industrial growth have intensified air pollution in metropolitan regions, making accurate and energy-efficient Air Quality Index (AQI) prediction critical for sustainable smart city management. Existing centralized and conventional federated learning approaches suffer from high communication overhead, excessive energy consumption, and privacy risks, limiting their applicability in distributed urban sensing environments. This paper proposes *GreenEdge AI*, a green federated learning framework integrating a green-aware custom LSTM (GA-CLSTM) model with energy-aware training, adaptive aggregation, and a hybrid loss function for decentralized AQI forecasting. The framework enables edge-level learning across heterogeneous IoT-based air quality and meteorological sensors while preserving data privacy and minimizing cloud dependency. Sustainability is explicitly incorporated through green metrics, including energy consumption, Energy–Delay Product (EDP), Energy Efficiency Ratio (EER), and Power-to-Performance Ratio (PPR), which guide both model optimization and federated aggregation. Experimental results on real-world hourly AQI data from five major metropolitan

	cities demonstrate that *GreenEdge AI* achieves up to 60% improvement in prediction accuracy and approximately 37% reduction in energy consumption compared to conventional baseline models, while significantly reducing peak power usage and communication overhead compared to centralized and conventional federated baselines. These findings underscore the practical value of *GreenEdge AI* for municipalities and environmental agencies, motivating future research on scalable, energy-aware federated intelligence for smart city applications.
51.	Hierarchically structured organic cation intercalated heterojunction: A selective sensor–catalyst interface for simultaneous detection and degradation of fenitrothion Divya, S Kalra, N Kaur**, N Singh** - ACS Applied Engineering Materials, 2016 **Abstract:** The widespread use of organophosphate pesticides, especially Fenitrothion (FNT), in agricultural practices has raised serious environmental and health concerns. Even at trace levels, it can cause toxic effects through inhalation, ingestion, or dermal exposure, contributing to an estimated 2 million poisoning cases and 10,000 deaths annually. This growing threat highlights the urgent need for effective detection and remediation technologies. For this, we designed an organic cation (DM3)-intercalated interfacial heterostructure, DM3-ZnO/FeOCl. The selective response of DM3-ZnO/FeOCl toward the detection of FNT has been established through spectroscopic and electrochemical techniques. It acts as a smart FNT-responsive material that targets and degrades FNT from contaminated water and soil. Moreover, a cost-effective DM3-ZnO/FeOCl-embedded poly(vinyl alcohol)/polyethylene glycol matrix (FenitroPur) has been developed as a portable system for the degradation of FNT in real-world scenarios. Mechanistic insights reveal that the degradation of FNT follows pseudo-first-order kinetics, achieving >99% degradation through a Recognize-Catalyze-Degrade mechanism. The role of radical species has been studied by using radical scavenger assays, and consequently, a degradation pathway has been evaluated. This work provides an environmentally friendly and sustainable solution for FNT removal from soil and water, thereby ensuring overall well-being. 
52.	High-index dielectric metasurfaces: Unlocking frontiers in mid-infrared photonics **D Vishnuramkumar, D Singh** - ACS Applied Optical Materials, 2026 **Abstract:** Metasurfaces, engineered planar structures manipulating light at subwavelength scales, have revolutionized nanophotonics across the visible to terahertz spectrum. All-dielectric material-based metasurfaces offer low optical losses, CMOS-compatible fabrication, and efficient light control via electric and magnetic resonances. The refractive index of such materials critically impacts the device performance, as traditional semiconductors like silicon and germanium provide moderate confinement, while emerging high-index materials such as WS_2, PbTe, and GeSbTe enable stronger field localization and smaller device footprints. These high-index materials are vital for compact, reconfigurable metasurfaces operating in the mid- to far-infrared, essential for sensing, imaging, and thermal control. This article focuses on mid-IR photonics with dielectric metasurfaces, highlighting materials for high to ultrahigh refractive index with low losses, their advantages over plasmonics, and applications in wavefront control, nonlinear optics, and tunable devices. Future perspectives include scalable fabrication, AI-driven design, and broad industrial impact.

	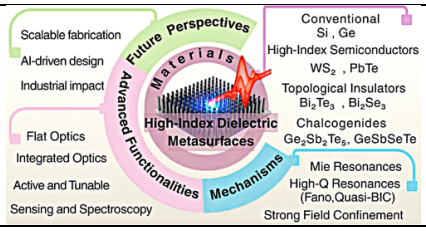
53.	Hydrophobic PEACl additive for low-temperature processed all-inorganic $CsPbIBr_2$ perovskite solar cells N Chandrakar, **M Kumar,** DP Singh - Materials Letters, 2026 **Abstract:** Low-temperature fabrication of $CsPbIBr_2$ perovskite film leads to defect site trap formation, thereby impeding the crystallization of $CsPbIBr_2$ films. In this report, we have investigated phenethyl ammonium chloride (PEACl) as an additive in $CsPbIBr_2$ perovskite. The incorporation of PEACl effectively modulates perovskite crystallization and suppresses defect formation, as evidenced by the enhanced morphology and improved crystallinity of $CsPbIBr_2$ perovskite films. As a result, the optimized PEACl additive $CsPbIBr_2$ PSCs achieve a power conversion efficiency (PCE) of 8.43% and an open-circuit voltage (V_{OC}) of 1.17 V, with an active area of 0.25 cm^2. The stability of unencapsulated devices were tested under ambient conditions (~27 °C, 45–65% relative humidity).
54.	lgarIntegrated bidirectional electric vehicle battery network for sustainable communities: A planning framework S Sekar, **AS Tiwana,** KS Grewal - Green Energy and Intelligent Transportation, 2025 **Abstract:** The transition towards sustainable and net-zero energy communities has become imperative in addressing the challenges of climate change and ensuring a resilient energy future. This work proposes an innovative planning framework through the development of an integrated bidirectional electric vehicle (EV) battery storage network for net-zero communities. The proposed framework is intended for neighborhood planning and integrates a bidirectional charging infrastructure that allows EV batteries to seamlessly contribute to the grid during periods of high demand or store excess renewable energy during off-peak hours. To analyze various EV microgrid integration scenarios, a combined Matlab-Simulink and EnergyPlus simulation environment is proposed to simulate EV battery networks in neighborhood settings. This study examines state of charge (SoC), and energy exchange characteristics based on specific user behaviors and charging scenarios. A neighborhood archetype of 48 single-family detached houses is considered along with five EV use profiles (EVPs) for the demonstration of the proposed method. For the considered neighborhood, in winter, EVPs have eliminated the peak loads during early morning hours (1 am–6 am) by discharging stored energy. In spring, loads exceeding the base load are observed from 1 am to 10 am, with all EVPs discharging energy until 9 am and then recharging during off-peak hours. Summer required strategic charging management, with EVPs supporting peak loads from 7 am to 6 pm. In the fall, EVPs discharged energy from 12:01 am–6 am and recharged from 10 am to 6 pm. The study introduces the EVP peak support index facilitating real-time charging adjustments and incentivizing greater participation. By leveraging this index, smart charging systems can develop algorithms to control charging times based on grid needs, ensuring efficient energy distribution and enhanced grid stability. This framework offers a robust approach to scenario generation for energy and urban planners during the neighborhood planning stages predicting energy performance and management.

	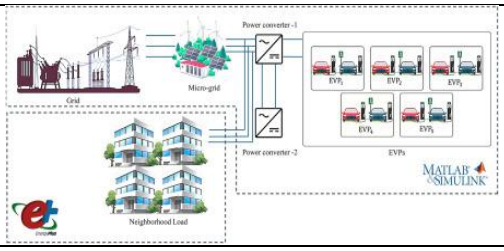
55.	Impact of nozzle injection angle on flow characteristics in cold spray process for hastelloy X superalloy powder **S Singh, L Palodhi, H Singh** - Journal of Thermal Spray Technology, 2026 **Abstract:** Hastelloy X exhibits excellent high-temperature strength and oxidation resistance, making it suitable for applications like including nuclear reactors, jet engines, and gas turbine engines. Conventional thermal spray techniques can induce thermal stresses, phase changes, and oxidation in Hastelloy X deposits. Cold spray is a solid-state technique that enables the deposition of dense, oxide-free coatings while maintaining the alloy's original microstructure. This numerical study investigates the impact of various powder injection angles (0°, 30°, 60°, and 90°) on the cold spray process for Hastelloy X superalloy powder. Using computational fluid dynamics (CFD), we analyze particle velocity and flow characteristics to identify the optimal injection angle. The selected turbulence model, k-ω SST, effectively characterizes turbulent flows, making it suitable for elucidating the dynamics of gas-particle interactions. Complex flow structures, including Mach diamonds and shock waves, were observed, creating alternating pressure and velocity fields that significantly affect particle momentum transfer. Among all cases, the 30° injection angle achieved the highest particle velocity and the most focused particle stream, enabling more efficient entrainment and mixing. It also showed the most focused particle stream. Experimental validation using Accuraspray CS recorded an in-flight particle velocity of 710 ± 20 m/s 30° powder injection angle, in good agreement with the CFD-predicted 765 m/s. Microstructural analysis of deposited coatings revealed dense Hastelloy X layers with low porosity (0.70% ± 0.02%) and high deposition efficiency (92%). These results demonstrate that injection-angle optimization is critical for achieving superior particle acceleration and coating quality in cold spray of Ni-based superalloys.
56.	Influence of stoichiometric variation of 3d-4d transition metal ions in disordered double perovskite for bifunctional electrocatalysis T Rom, A Chakraborty, **K Garg,** E Lee, HC Ham, **TC Nagaiah,** AK Paul - Chemistry of Materials, 2026 **Abstract:** In pursuit of an efficient and sustainable energy conversion system, the design and development of an advanced bifunctional electrocatalyst for overall water splitting offers a promising approach for producing renewable hydrogen fuel. However, integrating bifunctionality into a single catalyst remains a considerable challenge, especially for materials derived from double-perovskite oxides. In this regard, three phase-pure polycrystalline disordered double-perovskite oxides, i.e., Ca_2MnRuO_6 (CMR), $Ca_2Mn_{1.25}Ru_{0.75}O_6$ (CMR-1), and $Ca_2Mn_{0.75}Ru_{1.25}O_6$ (CMR-2), are synthesized to assess their potential as bifunctional electrocatalysts and evaluate the impact of mixed-valence 3d-4d transition metal ions (Mn/Ru) on the electrocatalytic performance of water splitting. Among the title compounds, the as-synthesized CMR-2 catalyst demonstrates remarkable hydrogen evolution reaction (HER) activity in an alkaline medium (1 M KOH) and shows a minimal overpotential of 270 mV at 10 mA/cm^2, outperforming both CMR (η_{10} = 328 mV) and CMR-1 (η_{10} = 280 mV) catalysts. Furthermore, when assessed for oxygen evolution reaction (OER) in the same electrolyte medium, the CMR-2 catalyst requires a very small overpotential of 300 mV @10 mA/cm^2 compared to the benchmark RuO_2 and various well-engineered oxide-based electrocatalysts with an F.E. of 77% at 1.62

	V *vs* RHE. Coupled with its efficient and robust bifunctional catalytic performances, a prototype two-electrode-based water electrolyzer (H cell) was assembled with the CMR-2 catalyst, used as both the anode and cathode to perform overall water splitting studies. The fabricated water electrolyzer exhibits a comparable cell voltage and long-term stability, with negligible degradation over 24 h of continuous operation in a 1 M KOH electrolyte, highlighting its promising potential for future practical application. Moreover, the compelling composition-activity behaviors and detailed mechanistic investigations of the present disordered double perovskites are also corroborated by density functional theory (DFT) calculation studies. 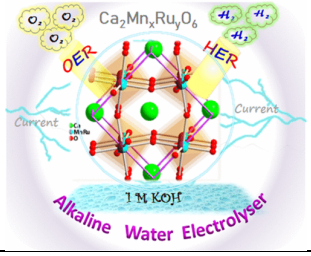
57.	LearnRouter: A reinforcement learning-based routing for opportunistic mobile networks using multi-armed bandit approach **A Phutela, S Koshta, S Pal,** S Sampalli - IEEE Transactions on Mobile Computing, 2025 **Abstract:** Efficient routing protocols are required in opportunistic networks due to the inherent challenges of sporadic connectivity, transmission delays, and dynamic network topologies. In these networks, information is forwarded and disseminated among smart devices based on opportunistic contacts driven primarily by network dynamics and user mobility. This paper introduces LearnRouter, a dynamic reinforcement learning-based routing algorithm designed to improve the message delivery ratio while minimizing end-to-end delay in opportunistic networks. Existing routing protocols use static strategies or fixed replication schemes, leading to resource utilization and high message drop rates. LearnRouter addresses these challenges by incorporating the multi-armed bandit framework and utilizing the Upper Confidence Bound algorithm to make more intelligent and data-driven forwarding decisions. The proposed approach enables the protocol to adapt continuously to network changes while balancing the trade-off between exploration and exploitation. The simulation results show that LearnRouter surpasses end-to-end delay and message delivery ratio in comparison with Direct Delivery, Spray and Wait, CBR, SimRouter, RL-Prophet, and K-DQLR in opportunistic and dynamic environments.
58.	Manganese-copper-gallium alloys for sustainable refrigeration through a synergistic study of magnetocaloric and mechanical behavior N Tiwari, S Mishra, **A Kumar,** VK Malik, **D Roy,** M Paliwal, V Chaudhary, AK Singh - Advanced Engineering Materials, 2026 **Abstract:** Emerging solid-state refrigeration holds great promise for improving energy efficiency and reducing greenhouse gases, thereby supporting sustainable systems. However, the challenge lies in identifying magnetocaloric materials that possess the necessary properties for real-world applications. Currently, there is a scarcity of materials that exhibit the ideal combination of magnetocaloric effects, mechanical properties, and minimal thermal hysteresis, which are essential for practical applications. The present study explores Mn-Cu-Ga-based alloys for magnetocaloric applications to address all three challenges. Alloy compositions are selected based on CALculation of PHAse diagrams calculations and experimental evaluation of magnetocaloric and mechanical properties. The optimal change in magnetic entropy is 2.84 J kg^{-1}-K^{-1}, and refrigeration capacity is 115.2 J kg^{-1} at a 2 Tesla magnetic field. The thermal hysteresis, a factor that enhances the practical viability of the investigated alloys, is 1 K. Mechanical testing is performed to explore the ductile behavior of the investigated alloys. The strain-hardening exponent (n) indicates that the

	ductility is between 0.30 and 0.38, indicating a ductile nature. To support the experimental findings, first-principles calculations are performed. This dual approach, combining experimental and theoretical methods, offers a comprehensive understanding of Mn-Cu-Ga alloys for magnetocaloric applications.
59.	Maximal independent set via leader election by mobile agents from arbitrary initial configuration without global knowledge **T Kaur,** B Gorain, **K Mondal** - SN Computer Science, 2026 **Abstract:** We consider the problem of finding a maximal independent set (MIS) of an unknown graph by mobile agents. Let n agents be initially positioned arbitrarily at the nodes of an anonymous graph. The agents reposition themselves to achieve a configuration that forms an MIS of the graph, and terminate. Our algorithm solves the problem and achieves termination in rounds utilizing memory per agent. The agents do not have any prior knowledge of any graph parameters. Additionally, we solve the leader election problem during the process. From the MIS perspective, our result improves over Pattanayak et al. (ICDCN 2024) by removing global knowledge as well as by reducing run time. We improve over Kshemkalyani et al. (DISC 2024) by reducing memory requirement as well as runtime. This is because authors provide a runtime of where is the maximum degree of the graph and it can be asymptotically more than our runtime whenever the average degree is much lesser than the maximum degree. Due to the same reasoning our time complexity is better compared to the runtime of MIS finding in Kshemkalyani et al. (AAMAS 2025) as well.
60.	Measurement of volumetric current and estimation of nonlinear dielectric impedance of LDPE **C Iyyappan, P Muppala, CC Reddy** - IEEE Transactions on Instrumentation and Measurement, 2026 **Abstract:** In low-density polyethylene (LDPE) insulation, the nonlinear nature of volumetric current–time characteristics was often attributed to its complex space charge dynamics, apart from temperature and electric field dependence. However, a scant attention is given to the measurement-related issues of volumetric current in the literature. In this article, we have presented experiments conducted on measuring circuits used in electrometer as well as with the commercial electrometer to investigate the measurement-related aspects on the current characteristics of LDPE. Matching the time constants of measuring circuit impedance with the dielectric under test would typically offset all the errors of the measurement. However, LDPE, with the nonlinear variation of its impedance characteristics, makes it difficult for accurate measurement, as it dynamically deviates from the fixed time constant of the measuring circuit impedance. Hence, the true volumetric current characteristics and a novel circuit model for the impedance of LDPE are proposed. Interestingly, they are observed to corroborate well with the transient space charge limited current (TSLC) theory.
61.	Mechanics-guided parametric modeling of intranasal spray devices and formulations for targeted drug delivery to the nasopharynx MT Hossain… **D Samanta**… S Basu - Frontiers in Drug …, 2025 **Abstract:** Introduction: Improving the efficacy of nasal sprays by enhancing targeted drug delivery to intra-airway tissue sites prone to infection onset is hypothesized to be achievable through an optimization of key device and formulation parameters, such as the sprayed droplet sizes, the spray cone angle, and the formulation density. This study focuses on the nasopharynx, a primary locus of early viral entry, as the optimal target for intranasal drug delivery. Methods: Two full-scale three-dimensional anatomical upper airway geometries reconstructed from high-resolution computed tomography scans were used to numerically evaluate a cone injection approach, with inert particles mimicking the motion of sprayed droplets within an underlying inhaled airflow field of 15 L/min, commensurate with relaxed breathing conditions. Therein we

	have considered monodisperse sprayed particles sized between 10–50 (Formula presented.) m, six material densities ranging from 1.0–1.5 g/mL for the constituent formulation, and twelve plume angles spanning 15 (Formula presented.) – 70 (Formula presented.) subtended by the spray jet at the nozzle position. Large Eddy Simulation-based modeling of the inhaled airflow physics within the anatomical domains was coupled with a Lagrangian particle-tracking framework to derive the drug deposition trend at the nasopharynx. Results: The resulting three-dimensional deposition contour map, obtained by interpolating the outcomes for the discrete test parameters, revealed that the mean nasopharyngeal deposition rate peaked for particle sizes (Formula presented.) [25, 45] (Formula presented.) m and plume angles (Formula presented.) 30 (Formula presented.), with the deposition rates averaged over the test airway geometries and formulation densities. That mean deposition rate at the nasopharynx was approximately 11.4% within the specified (Formula presented.) parametric bounds. In addition, the formulation density of 1.0 g/mL yielded the highest mean deposition rate, over the comprehensive tested range of sprayed particle sizes and plume angles. A subset of the simulated nasopharyngeal deposition trends was experimentally validated through representative physical spray tests conducted in a 3D-printed replica of one of the test geometries. Discussion: The overall findings, while implicitly tied to the two test subjects (i.e., for spray administration through four representative nasal pathways), do collectively demonstrate that rational optimization of the intranasal sprays for targeted nasopharyngeal deposition is attainable with actionable design modifications on the sprayed droplet sizes and device plume angles.
62.	Mechanistic insights into graphene oxide-enhanced single electrospun PMMA fibres achieved via surface interface engineering AS Bhat, **JA Malik**… **JN Agrewala,** SK Tiwari - Materials Advances, 2026 **Abstract:** Herein, we focus on optimising the electrospinning parameters to fabricate well-defined, physically distinct cotton-like fibres of polymethyl methacrylate (PMMA) with the incorporation of 0.39 wt% graphene oxide (GO). So-fabricated cotton-like distinct single fibres were extensively characterised by employing advanced techniques like high-resolution transmission electron microscopy (HRTEM) to study the internal structure and atomic force microscopy (AFM) to evaluate the mechanical properties of the single fibres at the nanoscale to overcome the ambiguities associated with the conventional mechanical property testing for a fibrous mat. The studies revealed that the fibres produced were highly flexible (DMT modulus ~ 0.28 GPa) with exceptional thermo-mechanical performances and cryogenic stability. Also, the probable underlying mechanism and the molecular-level interaction of PMMA–GO have been discussed thoroughly. The biocompatibility of PMMA–GO single fibres has been examined by the cell viability test. The findings demonstrated that PMMA–GO fibres are non-toxic to cells at higher GO concentrations. Importantly, this study is directed towards the comprehensive characterisation of single electrospun fibres, thereby investigating their behaviour in a cryogenic (liquid nitrogen) environment.
63.	Multifunctional SrFe2O4 nanoparticles: Structural, optical, and magnetic insights with potent cytotoxicity against mcf-7 breast cancer cells M Kaur, **A Singh,** MS Sankhla, AK Tangra - Journal of the Indian Chemical Society, 2026 **Abstract:** Magnetic nanomaterial $SrFe_2O_4$ with excellent biocompatibility has emerged as a promising candidate for biomedical applications, particularly in cancer diagnostics and therapy. The structural, optical, magnetic, and biocompatible characteristics of the $SrFe_2O_4$ nanoparticles, which were synthesized by using sol-gel process, were thoroughly examined. The monoclinic crystal structure of the sample, belonging to the $P2_1/c$:c2 space group, was confirmed by X-ray diffraction (XRD) analysis. Morphological analysis of the syntheized nanoparticle is done by using Transmission electron microscopy (TEM) showed that the nanoparticles possessed a spherical shape, with an average particle size of ~24 nm. Magnetic measurements confirmed

	superparamagnetic behaviour at 300 K temperature, with a saturation magnetisation of 43 emu/g. Optical studies complemented structural insights by revealing band gap of ~2.84 eV which is correlating the crystallinity with the results obtained from TEM and XRD analysis. Furthermore, the SRB assay was used to evaluate biocompatibility in MCF-7 breast cancer cells treated with $SrFe_2O_4$ nanoparticles, which showed a concentration dependent decrease of cell viability, suggesting low cytotoxicity and favourable interaction with biological systems. These multifunctional properties make $SrFe_2O_4$ nanoparticles highly attractive for future applications for biomedical applications. 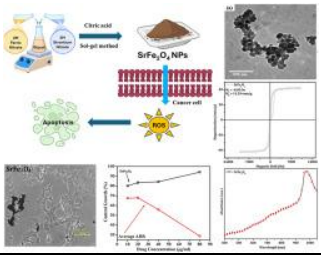
64.	NiO nanoflowers for non-enzymatic amperometric detection of glucose P Choudhary, C Chetiwal, **VK Singh,** A Dixit - Journal of Visualized Experiments (JoVE), 2025 **Abstract:** Non-enzymatic glucose sensors employing nanostructured metal oxide materials are amongst the most extensively researched topics currently. Several transition metal oxides (TMOs), such as iron oxides (α-Fe_2O_3, γ-Fe_2O_3, Fe_3O_4, etc.), nickel oxide (NiO), copper oxide (CuO), chromium trioxide (CrO_3), etc., have been utilized as enzyme-mimicking catalysts for glucose oxidation. Along with the use of different TMO materials, considerable efforts have been put into studying the impact of different morphologies of these materials. The literature shows that the flower and wire-shaped catalysts perform better due to their large surface area. This study presents the non-enzymatic glucose sensing properties of NiO nanoflower decorated glassy carbon electrodes (NiO NF@GCE). The central objective of this work is to shed light on the processes involved in the fabrication and characterization of glucose-sensing NiO nanoflowers on GCE. The amperometric detection of glucose shows a linear increase in current over physiologically relevant glucose concentrations ranging between 0 mM and 15 mM. The electrodes offer an excellent sensitivity of 281.69 $\mu A\ mM^{-1} \cdot cm^{-2}$ and a limit of detection of 10 μM. The results show that the linear range of detection increases while the sensitivity decreases with an increase in the loading mass of the nanomaterial after a certain loading concentration. In addition, the electrodes showed high selectivity towards glucose in the presence of other interfering species, such as ascorbic acid, fructose, sucrose, and NaCl. The impact of loading concentration on the selectivity of NiO NF-modified electrodes shows a decrease in selectivity with the increase in loading of the nanomaterial after a certain optimal loading mass.
65.	Non-destructive, non-invasive infrared thermography technique in rock mechanics for early prediction of rock failure **M Jaiswal, R Sebastian,** R Mulaveesala - ISRN (India) Journal, 2026 **Abstract:** Early prediction of rock failure remains one of the key challenges in rock mechanics and geotechnical engineering. Conventional destructive methods often compromise specimen integrity and limit their applicability for in-situ monitoring. In recent years, non-invasive infrared thermography (IRT) has emerged as a promising technique for capturing spatio-temporal temperature variations associated with microcracking and energy dissipation in rocks. This study reviews the theoretical background, experimental evidence, and practical feasibility of infrared thermography as a diagnostic tool for anticipating failure in rock materials. A framework is proposed for integrating IRT into laboratory testing and field monitoring, with emphasis on correlating thermal precursors with mechanical damage evolution. The approach holds potential

	for enhancing safety in underground construction, mining, and slope stability management, while contributing to the development of real-time monitoring systems.
66.	Palladium photocatalysis: A strategic approach for visible-light-mediated C (sp2)–H arylation **P Mistry, B Paul, V Ranga, I Chatterjee** - Chemical Communications, 2026 **Abstract:** A strategic and energy-efficient protocol has been developed to construct C(sp^2)–C(sp^2) bonds through C–H bond functionalization. Herein, Pd-photoredox catalysis under blue LED irradiation was used to generate aryl (or heteroaryl) radicals from the corresponding redox-active iodoarenes and utilize them in C–H bond arylation. The key attraction lies in the wide functional group tolerance with impressive yield and the late-stage functionalization of natural products under mild reaction conditions. Operational simplicity and mechanistic evidence for photoinduced Pd catalysis illustrate the promise of this approach as a comprehensive platform for sustainable aryl–aryl cross-coupling. 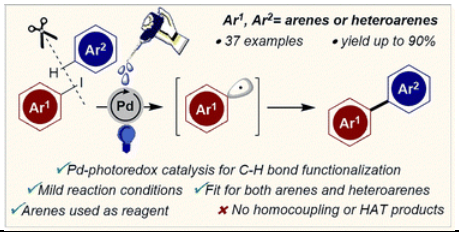
67.	Photocatalytic arylation of carbonyl compounds: Advancements toward sustainability **K Kaur, RD Thombare, P Singh, AC Shaikh** - Chemical Communications, 2026 **Abstract:** In recent decades, there has been a notable increase in interest surrounding the direct functionalization of carbonyl compounds, attributed to their extensive applications across various fields. However, conventional methodologies have predominantly relied on stoichiometric amounts of expensive and often environmentally detrimental metal oxidants, which present significant sustainability challenges in the arylation processes. In contrast to traditional transition metal-catalysed arylations, photochemical methods offer environmentally friendly reaction profiles, greater operational simplicity, and access to novel reactivity modes that are not achievable under thermal conditions. This review highlights recent advancements in visible-light-driven arylation techniques that enable the formation of carbon–carbon (C–C) bonds at either the α- or the β-position, or directly at the carbonyl center of carbonyl compounds. The tutorial review also emphasizes the mechanistic insights, including radical chain propagation, proton-coupled electron transfer (PCET), and energy transfer pathways, that underpin these transformations. By leveraging the potential of photocatalysis, particularly through single-electron transfer (SET) processes and radical-mediated mechanisms, these transformations demonstrate remarkable tolerance for a variety of functional groups and regioselectivity, even within challenging molecular structures by utilizing diverse arylating sources (including aryl diazonium salts, aryl halides, and cyanoarenes). The aim is to provide a concise overview of current methodologies, mechanistic insights, and future directions in photochemical arylation of carbonyl compounds, emphasizing its advancements toward sustainability in modern synthetic organic chemistry. This review summarizes advances in the photocatalytic arylation of carbonyl compounds, focusing on innovative strategies that promote sustainability.

	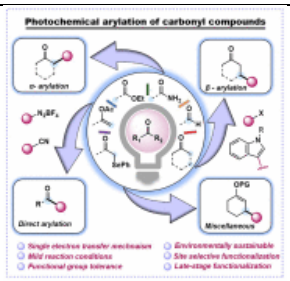
68.	Polarization controlled dual-polarized MIMO antenna with enhanced isolation for full-duplex WBANs **A Thakur, A Sharma,** IJG Zuazola - IEEE Open Journal of Antennas and Propagation, 2025 **Abstract:** A polarization controlled dual-polarized multiple-input multiple-output (MIMO) antenna with enhanced isolation for full-duplex wireless body area network (WBAN) in the 5.8 GHz industrial, scientific, and medical (ISM) band is proposed. The advanced polarization control of each antenna element comprising the MIMO antenna is realized by embedding tailored T-shaped strips within the transversal slots of a main diagonal cut in the ground plane, which effectively steer the surface currents to a favorable direction to achieve the desired polarization with enhanced isolation. By slotting the twin circular patch radiating elements and incorporating twin capacitively coupled stepped elements adjacent to their feeding terminals, the proposed low-profile design realizes good impedance matching, return loss, and bandwidth. Experimental results demonstrate isolation greater than 5 dB compared with existing designs, and we report inter-port isolation that exceeds 33 dB for the 150 MHz bandwidth, with a peak isolation of approximately 67 dB. As a result, the proposed antenna exhibits low envelope correlation coefficient (ECC), high diversity gain (DG), and acceptable total active reflection coefficient (TARC) and channel capacity loss (CCL). A prototype antenna was tested under structural deformation by bending it along a -45∘ direction, with a simulated specific absorption rate (SAR) of 0.258 W/kg on a human phantom, thereby validating the antenna's compliance with safety standards. The findings of this study demonstrate that the proposed design effectively addresses critical challenges in full-duplex WBAN antennas by enhancing port isolation, minimizing mutual coupling, and advancing polarization control, while maintaining a low-profile and low-complexity feeding network structure.
69.	Productive chaos and precision engineering: Decoupling discovery from manufacturing to revolutionize plant-inspired therapeutics **DA Mosoh** - Frontiers in Plant Science, 2026 **Abstract:** The pharmaceutical industry remains critically dependent on plant-derived natural products, yet the supply of these complex molecules is perpetually threatened by the inherent biological instability of plant systems. For decades, the field has struggled to force undifferentiated plant cell cultures into the mold of consistent industrial fermentation, a strategy largely defeated by epigenetic drift, somaclonal variation, and a linear cost structure that prohibits pharmaceutical scalability. This literature-based review articulates a fundamental paradigm shift: the strategic decoupling of discovery from production. It argues that the genomic plasticity of plant cells should not be suppressed but rather induced through stress elicitation to generate a "productive chaos" of chemical diversity for discovery. This expanded metabolic landscape is then decoded using single-cell multi-omics to identify elite producer cells, alongside advanced artificial intelligence and molecular networking to characterize novel bioactive candidates. Once identified, these pathways are repatriated into defined, heterologous microbial hosts, engineered via systems-level architectural optimization—including cofactor balancing and P450-reductase stoichiometry—for stable, high-titer manufacturing. By integrating techno-economic analysis, multi-omics, machine

	learning-guided strain optimization, and automated biofoundries, this "discovery-production decoupling" resolves the tension between biological complexity and industrial rigor. This framework transforms the economics of natural product supply, transitioning from the low-CAPEX/high-OPEX trap of extraction to the high-CAPEX/low-OPEX scalability of fermentation, offering a scientifically robust, commercially viable, and regulatory-compliant pathway to unlock the full therapeutic potential of the plant kingdom.
70.	Progressive impact of polycystic ovary syndrome on hormonal alterations, bone microarchitecture, and mechanical properties S Pandey, **S Kumar**… **N Kumar**… M Arshad - Journal of Endocrinology, 2026 **Abstract:** Polycystic ovary syndrome (PCOS) is characterized by reproductive and metabolic dysfunction that may also impact bone metabolism and its structural integrity. This study aims to assess the progressive impact of PCOS on bone health over time. It focuses on how the duration of the condition influences hormonal profiles, bone metabolism, and bone's microstructural and mechanical properties in the PCOS-induced mice model. Female BALB/c mice were separated into three groups, each further subdivided into PCOS-induced and age-matched control groups. PCOS was induced by letrozole (6 mg/kg b.w.) administered continuously for 21 days; among them, group II underwent a one-month observation period, while group III was observed for two months. Bone quality markers were assessed through hormonal profiling, serum bone turnover markers, micro-CT, three-point bending test, nanoindentation, and FTIR. Hormonal profiling revealed persistent hyperandrogenism, elevated luteinizing hormone/follicle-stimulating hormone ratio, reduced estrogen levels, and insulin resistance collectively affected bone health. Micro-CT analysis showed a decline in trabecular quality in the femur and tibia of the PCOS group. Three-point bending test pointed toward increased susceptibility to micro-damage and fracture. Nanoindentation indices, elasticity, and hardness were also decreased. FTIR analysis indicates alterations in bone material properties. These indices showed a slight improvement in the third month but deviated significantly from control. Our results suggest that PCOS has an adverse impact on bone's structural, mechanical, and compositional properties, and the negative impact of PCOS on skeletal integrity is not fully reversible in the short term. Overall, these findings highlight the importance of evaluating and monitoring bone health in PCOS individuals.
71.	Patterns of alcohol use and response to digital brief interventions in college students: a secondary analysis of a cluster randomized trial A Ghosh… **A Kumar,** D Basu, MP Schaub - Frontiers in Psychiatry, 2025 **Abstract:** Background: Drinking among college students in India is rising, influenced by social and cultural shifts. This study aimed to classify drinking behaviors among underage students using Latent Class Analysis (LCA) and assess the effectiveness of digital screening and brief intervention (DSBI) and brief advice (DSBA) across identified classes. Methods: This was a secondary analysis of a two-stage cluster randomized trial that screened 693 college students (age 18–22 yrs) with the Alcohol Use Disorders Identification Test (AUDIT). LCA was employed to identify latent classes in a main sample (N = 693, AUDIT ≥1) and a subsample of enrolled participants (N = 548, AUDIT scores 8-19). Model fit was assessed using AIC, BIC, and log-likelihood values, with a 3-class solution preferred for its interpretability and fit. A General Linear Model (GLM) analyzed the effectiveness of digital interventions over 3 and 6 months. Results: Three latent classes emerged from the main sample: "recreational drinkers" (minimal issues), "hidden problem drinkers (limited family concerns)," and "problem drinkers" (higher family concerns). In addition to the "hidden problem drinkers", the subsample comprised "emerging" and "observable" problem drinkers. Significant reductions in AUDIT scores were observed across all classes from baseline to 3 months, which stabilized by 6 months. A significant interaction effect was found between time and latent class [F (4) =14.60, p<.0001], "observable problem drinkers"

	outperforming the two other classes. Conclusions: Underage drinking represents three latent classes. Digital interventions can effectively reduce alcohol use across all classes of underage college problem drinkers.
72.	Room-temperature superprotonic conductivity in COOH-functionalized multicomponent covalent organic frameworks G Chakraborty, **P Das,** B Bhattacharya, C Prinz, F Emmerling, A Thomas - Chemical Science, 2026 **Abstract:** In solid materials, the development of hydrogen bonding (H-bonding) networks within pores is crucial for efficient proton conductance. In this study, a chemically stable carboxylic acid-functionalized, quinoline-linked 2D microporous covalent organic framework (COF) (Qy-COOH) was synthesized using the Doebner multicomponent reaction (MCR) and compared to a similar framework lacking the –COOH functionality (Qy-H), prepared *via* an MC Domino reaction. The proton conductivity of the –COOH-functionalized MCR-COF was significantly enhanced, reaching 10^{-2} S cm^{-1}, attributed to strong H-bonding interactions between water molecules and the dangling –COOH groups within the COF pores. In contrast, the analogous Qy-H framework exhibited a much lower proton conductivity of 10^{-5} S cm^{-1}, while an imine-based COF showed only 10^{-6} S cm^{-1}. This work represents the first demonstration of a general strategy to achieve efficient proton conduction in a class of layered 2D –COOH-functionalized COFs, offering superprotonic conductivity without requiring additives at room temperature. The MCR-COF design approach provides a promising pathway for developing highly stable and high-performance proton-conducting materials.
73.	Safe glucose regulation in artificial pancreas systems via robust control barrier functions S Saxena, **N Kumar** - Transactions of the Institute of Measurement and Control, 2025 **Abstract:** Artificial pancreas systems (APSs) have transformed insulin delivery for individuals with Type 1 Diabetes Mellitus. However, these systems remain vulnerable to both physiological disturbances (meal) and cyber-physical threats such as Denial-of-Service (DoS) attacks that block insulin delivery actuation channel. This work presents a robust control framework using control barrier functions (CBFs) to enforce glucose safety constraints without violating hyper- or hypoglycemia, even under attack-induced uncertainties. We develop both standard and robust CBFs based on the physiological model of glucose-insulin interactions. We introduce a novel insulin-adaptive safety filter that anticipates delayed insulin action for improved closed-loop response. The proposed method guarantees for forward invariance and input-to-state safety. To counteract actuation-layer DoS attacks, we propose a fallback defense mechanism. Simulation results demonstrate the effectiveness of the proposed approach in maintaining glucose levels within safe bounds, ensuring resilience and reliability in APS operation.
74.	Similar but different: ERP evidence on the processing of mental and physical experiencer verbs in Malayalam **S Shalu,** R Muralikrishnan, **AM Mathew, KK Choudhary** - Frontiers in Language Sciences, 2025 **Abstract:** This study investigated the neurophysiological correlates of processing mental and physical subject experiencer verbs in Malayalam. Event-related brain potentials (ERPs) were recorded as 28 first-language speakers of Malayalam read intransitive sentences with the two types of experiencer verbs. Critical stimuli were either fully acceptable, whereby the subject case matched the requirements of the verb, or unacceptable, whereby the subject case violated the requirements of the verb. A linear mixed-models analysis confirmed negativity effects in the time window 400–800 ms for mental and physical experiencer verbs. Post-hoc analyses revealed that the negativity peaked relatively early for mental experiencer verbs, whereas relatively late for

	physical experiencer verbs. Further, the sentence-final acceptability of trials modulated the ERPs in non-anomalous conditions but not in violation conditions, and this modulation qualitatively differed between mental and physical experiencer verbs. These results suggest that, whilst a qualitatively similar mechanism is involved in the processing of both kinds of experiencer verbs, subtle but robust differences are inherent in processing mental vs. physical experiencer verbs in Malayalam.
75.	Some insights into the ratcheting behavior of P91 steel at elevated temperature **R Dhiman, SC Roy** - Fatigue & Fracture of Engineering Materials & Structures, 2025 **Abstract:** This article highlights the importance of "opening strain," which quantifies the amount and direction of net cyclic plastic deformation, in describing the ratcheting behavior of materials. Ratcheting experiments were conducted on P91 steel at 823 K with varying stress amplitude (290–380 MPa) and mean stress (0–120 MPa). Analysis revealed that ratcheting occurs due to unequal cyclic tensile and compressive plastic strains, leading to non-closure of hysteresis loops, quantified as "opening strain." The ratcheting behavior of P91 steel exhibited an initial quasi-stable phase followed by an acceleration phase before failure. Transmission electron microscopic investigation of interrupted test specimens highlighted that dislocation tangles, forests, and networks were associated with minimal strain accumulation in the stable phase. Further investigation of the failed specimens confirmed that the formation of incipient dislocation cells and recrystallized subgrains provided strain-free paths for dislocation motion and significant strain accumulation in the acceleration phase.
76.	SpinVision: An end-to-end volleyball spin estimation with Siamese-based deep classification **S Bansal,** AK Bedi, P Kumari, **RK Soni,** N C Krishnan, **M Saini** - Computer Vision and Image Understanding, 2025 **Abstract:** Accurate spin estimation is a very crucial process in detailing ball dynamics, conducting trainings and analyzing performance in different sports such as volleyball. Traditional methods usually rely on geometric assumptions, handcrafted features, or marker based estimation, which leads to their limited adaptability to real-world problems. In this paper, we propose a novel spin estimation framework, namely SpinVision, considering it as a soft-classification problem. The deep learning model employs Gaussian soft labels and Kullback–Leibler Divergence (KLD) loss. Further, it employs fusion methods alongside squeeze-and-excitation blocks and residual connections, which helps in achieving distinctive representations without the support of external markers or registration procedures. Also, inclusion of transfer learning helps generalizing the model effectively to real-world problems, such as estimating the spin of a volleyball. When compared with the hard-classification or regression-based methods, the proposed model results in more reliable and smooth predictions, thus highlighting it as more accurate, robust, and practical solution for spin prediction in sports analytics and related applications. 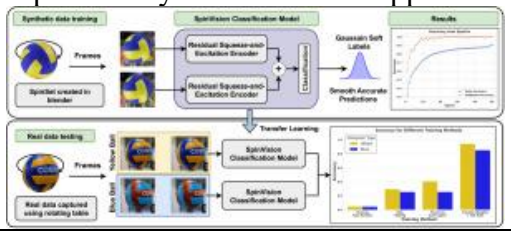
77.	Structural, morphological, and nonlinear optical characteristics of NiO thin films prepared by electron -beam evaporation Minakshi… **G Kumar,** PS Patil – Journal of Materials Science Materials in Electronics, 2026 **Abstract:** Nickel oxide (NiO) nanostructures were synthesized by thermally oxidizing thin nickel (Ni) films deposited on glass substrates via electron beam evaporation under a controlled vacuum

	environment. Thermal oxidation was performed at 400 °C, 500 °C, and 600 °C in ambient air. X-ray diffraction (XRD) confirmed mixed phases of Ni and NiO at 400 °C and 500 °C, whereas a single-phase NiO with improved crystallinity was obtained at 600 °C. XRD data were analyzed using Rietveld refinement to confirm phase composition and structural evolution. Field emission scanning electron microscopy (FESEM) revealed that higher oxidation temperatures promote grain growth and induce a porous morphology. Energy-dispersive X-ray spectroscopy (EDX) confirmed the chemical purity of the oxidized films, showing only nickel and oxygen. Optical absorption analysis demonstrated a redshift in the bandgap with increasing temperature, consistent with defect-mediated electronic transitions. X-ray photoelectron spectroscopy (XPS) of the Ni 2p core level exhibited characteristic Ni $2p_{3/2}$ and Ni $2p_{1/2}$ peaks along with satellite features, evidencing the coexistence of Ni^{2+} and Ni^{3+} oxidation states. Nonlinear optical behavior was probed using the Z-scan technique at 532 nm, yielding third order nonlinear susceptibility ($\chi 3$) values in the range of 3.64×10^{-4}–1.67×10^{-4} esu. The films displayed strong nonlinear absorption and thermal lensing effects, with an optical limiting threshold as low as 0.26 kJ/cm^2. These findings highlight the potential of NiO thin films as efficient candidates for nonlinear optical limiting applications, where structural tuning via oxidation temperature plays a critical role in enhancing performance.
78.	Sustainable, flexible and ambient temperature operated polyaniline-based chemiresistive ammonia sensor with eco-friendly design A Beniwal, **R Gond,** X Karagiorgis, **B Rawat,** C Li - IEEE Sensors Letters, 2026 **Abstract:** In this work, an eco-friendly, flexible, and ambient temperature (~27 °C ± 2 °C) operated ammonia (NH3) sensor has been developed using electrospun polyaniline (PANI) fibers deposited on an eco-friendly paper substrate having printed graphene–carbon (G-C) interdigitated electrodes (IDEs). The sensor was designed to detect NH3 over a broad concentration range of 0.5–500 parts per million (ppm), targeting applications in environmental and healthcare monitoring. Structural, elemental, and morphological properties of the sensing layer were characterized using X-ray diffraction, energy-dispersive X-ray spectroscopy, and scanning electron microscopy, confirming the formation of well-aligned PANI fibers with entangled networks and rougher surface. The sensor exhibited excellent % response (1261% at 500 ppm), reproducibility, and good repeatability over multiple cycles. Selectivity studies showed a multifold % response toward NH3 gas as compared to interfering gases, such as CO2, CO, SO2, and NO2. The use of paper as a low-cost, eco-friendly substrate, combined with the scalable fabrication route, highlights the potential of this work for sustainable and disposable NH3 sensing platforms and environmentally-friendly sensing solutions. 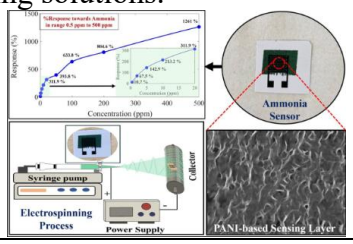
79.	Synergistic effect of sandwich layer of carbon nanotube bucky paper in carbon fiber reinforced hybrid laminated composite for high-performance mechanical and electromagnetic interference shielding J Jyoti, **A Kumar,** GS Chauhan, S Tripathy, BP Singh, KH Kim, N Kumar, SK Tripathi - Polymer Composites, 2026 **Abstract:** The fabrication of high-performance and lightweight composites is in huge demand, due to their excellent properties required for various applications. In this article, carbon fiber reinforced polymer (CFRP) laminated composites with different wt.% of carbon nanofillers and bucky paper fabricated from MWCNTs are interleaved, the mechanical and electrical performance

	of the composites are studied. The hybrid composites demonstrated outstanding mechanical properties and superior electromagnetic interference (EMI) shielding effectiveness. The X-ray computed tomography was used to determine the microstructure, delamination, and voids within the composites. The sandwich layer of BP/CFRP hybrid laminated composite showed significant improvement of 54.42% and 51.31% in flexural strength and flexural modulus respectively, compared to CFRP laminated composites. The BP reinforced interleaved CF reinforced hybrid laminated composites exhibited enhanced quasi-static dynamic mechanical properties. The storage modulus increased markedly for the sandwich-layered BCFRP (41.39 GPa), CBCFRP (40.14 GPa), and GBCFRP (31.76 GPa) composites, compared to that of only 19.74 GPa for the CFRP laminate composite. The shielding effectiveness in three frequency regimes was analyzed in the X, K, and Ku bands. The laminated composites exhibited total electromagnetic interference (EMI) shielding effectiveness values of 108.54 dB (BCFRP), 106.46 dB (0.3CCFRP), 105.38 dB (0.5GCFRP), and 104.67 dB (CFRP). Due to their outstanding mechanical and electromagnetic properties, the carbon nanofiller–interleaved CFRP laminated composites exhibit great potential for advanced civilian and military applications.
80.	Two-dimensional superconductivity: A review of computational approaches and emerging phenomena **P Jamwal, R Ahuja** and R Kumar - Nanotechnology, 2026 **Abstract:** Two-dimensional (2D) materials offer an exceptional platform for exploring quantum phenomena, as their reduced dimensionality significantly enhances tunability via external parameters. Among these, superconductivity in 2D systems is of particular interest due to its fundamental significance and potential applications in quantum technologies. Despite ongoing experimental challenges in realizing novel 2D superconductors, first-principles calculations have emerged as powerful tools for guiding their prediction and design. While many prior reviews focus broadly on low-dimensional superconductivity, this article specifically surveys computationally predicted 2D superconductors, with an emphasis on the underlying theoretical frameworks and their limitations. We highlight how external perturbations such as strain, doping, chemical functionalization, and intercalation, modify electron–phonon coupling and superconducting critical temperatures, and we examine cases where superconductivity competes or coexists with other quantum orders, including charge density waves and nontrivial band topology. We further discuss the growing role of machine-learning and high-throughput approaches in accelerating materials discovery, along with the challenges associated with data quality and model reliability. Overall, this review underscores the potential and current limitations of first-principles and data-driven approaches in advancing the understanding and discovery of 2D superconductors.
81.	Universal Ohmic contacts to β-Ga2O3 using interfacial dipoles of ultra-thin MgF2 layer and related defect passivation **Shivani, V Sheokand, Jiya,** CB Auti, P Kumar, **M Kumar** - Applied Physics Letters, 202 **Abstract:** We report on the role of MgF_2 as an interfacial buffer layer to achieve universal Ohmic contact on polycrystalline β-Ga_2O_3 thin film. Polycrystalline Ga_2O_3 thin films were deposited using RF magnetron sputtering, followed by the growth of MgF_2 through a modified approach within the same technique, enabling enhanced fluorination via trapped fluorine species. Three representative metals like Al (low work function ≈4.0 eV), and Ni, Au (high work functions ≈5.0 eV) were investigated to assess contact behavior. All three metals formed Schottky junctions with Ga_2O_3 in direct contact while insertion of an MgF_2 interlayer resulted in a clear transition to Ohmic conduction. Interface analysis using x-ray photoelectron spectroscopy (XPS) and Kelvin probe force microscopy (KPFM) revealed that fluorine incorporation passivates oxygen vacancies, reducing Fermi-level pinning, while Ga–F interfacial dipoles induce downward

	band bending. These combined effects effectively lower the Schottky barrier height enabling universal Ohmic contacts across metals with different work functions.
82.	Venturing into incremental forming of polycarbonate sheets through automated toolpath generation for improved industrial applications **M Pal, P Mahajan, A Agrawal** - Journal of Polymer Research, 2026 **Abstract:** Shaping of polymer sheets into complex shapes has been traditionally achieved using thermoforming process. However, for customized and complex geometries it is not economical to make dedicated moulds. Thus, Incremental Sheet Forming (ISF) has been explored for polymer sheet forming without the need of a dedicated moulds. ISF is a die-less and an adaptable manufacturing process, which offers unique advantages over other forming methods, due to its low tooling cost, rapid geometric customization, and the ability to form complex shapes through localized plastic deformation. Polycarbonate (PC), an engineering-grade amorphous polymer, is widely utilized for automotive, aerospace, and biomedical applications, etc., owing to its good impact resistance, optical transparency, and thermal stability. This work experimentally studies the formability of PC sheets with respect to the variation in the process parameters of incremental step depths and toolpaths during the ISF process. Furthermore, to improve the usability and industrial adoption of this process, a MATLAB®-based-graphical user interface (GUI) was developed, enabling users to input geometrical parameters, and generate different toolpaths to fabricate various geometrical 3D shapes. The study demonstrated that the spiral toolpath yielded higher tensile strength, better elongation through thermo-mechanical softening, and improved geometrical deformation compared to the conventional contour toolpath. Moreover, the smallest step depth of 0.1 mm assisted in achieving uniform surface finish with minimal tool markings on the formed part. With spiral strategy, lower average surface roughness of 0.97 μm were observed with lesser strain accumulation, relative to the contour, having the roughness of 1.4 μm. Whereas, increasing the wall angle from 30° to 60° also enhanced the viscoelastic material flow and surface quality with less deformation gradients, leading to higher formability and delay in localized fracture. Overall, these outcomes showed that with optimized parameters and incorporation of the GUI, can strengthen the potential of the ISF process for industrial-scale polymer forming applications.
83.	Virtual collagen mapping for quantitative microarchitectural analysis in whole-core pancreatic tissue microarrays **V Nair, G Uppal,** R Sinha, M Kaur, **S Gupta, R Kumar** - IEEE Journal of Selected Topics in Quantum Electronics, 2026 **Abstract:** Collagen remodelling plays a critical role in the progression of pancreatic intraepithelial neoplasia (PanIN) to pancreatic ductal adenocarcinoma (PDAC), though misdiagnosis often occurs due to the resemblance with chronic pancreatitis (CP). While second harmonic generation (SHG) microscopy is the current gold standard in research for visualizing fibrillar collagen, it is not utilized for routine histopathological use. This study highlights the need for an alternative method for quantitative collagen analysis that is compatible with standard hematoxylin-and-eosin (HE) stained histopathological slides. Using the computational image-to-image translation approach, whole-core standard brightfield HE images of pancreatic tissues were translated into the new collagen images. From these computationally translated collagen images, quantitative collagen measures were extracted for PDAC, PanIN, CP, and normal pancreatic tissues, and their statistical significance was evaluated. Among the four classes, PDAC tissues exhibited the highest collagen alignment ($n = 58$, $p < 0.01$, $R^2 = 0.2594$), while normal tissues showed the lowest fiber density ($n = 58$, $p < 0.0001$, $R^2 = 0.3569$). Seven machine learning models were assessed to differentiate neoplastic from non-neoplastic tissues cores based on collagen measures extracted from the translated collagen images. Feature importance and ROC-AUC analyses both identified fiber

	length and collagen deposition area as the most prominent parameters, achieving AUC values of 0.83 and 0.73, respectively, for distinguishing between the tissue classes. The findings demonstrate that the collagen images derived from standard HE-stained tissue microarrays (TMAs) whole-core images enable quantitative assessment of collagen remodelling across pancreatic lesions. Additionally, the study indicates that cross-modality image translation, as a cost-effective alternative, has the potential to offer deeper insights into histopathology and tissue microenvironment analysis without requiring collagen-specific imaging equipment or external labels, thereby further supporting its feasibility for integration into standard clinical workflows. 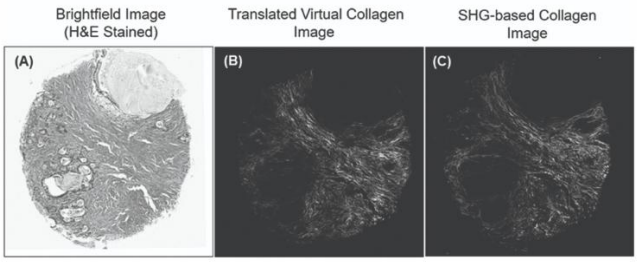
84.	Vulnerable options under a Hawkes jump-diffusion model with two-factor stochastic volatility **P Pasricha,** XJ He - International Review of Financial Analysis, 2026 **Abstract:** In this article, we address the valuation of a European vulnerable options within a structural framework. Specifically, we model the underlying asset and the asset of the option writer using a joint Hawkes jump-diffusion model with two-factor stochastic volatility. We derive a general analytical integral formula for prices of European options, applicable under any modeling framework as long as the joint characteristic function of asset prices associated with the underlying and option writer is available analytically. Distinguished from the pricing formulae in the literature, especially in a jump-diffusion framework, which is either in the form of the expectation over the jump process or requires evaluating several layers of infinite sums, our formula is significantly simplified and computationally efficient. Moreover, our model dynamics encompasses a wide range of commonly used models as special cases, for which we provide explicit analytical forms of the joint characteristic functions. Finally, we present numerical experiments demonstrating the accuracy and computational efficiency of our formula, along with sensitivity analysis to highlight the impact of various model parameters on the option prices.
85.	Warping labeling for twisted knots and twisted virtual braids **K Negi,** A Shimizu, P Madeti - Tokyo Journal of Mathematics, 2025 **Abstract:** In this paper, we introduce the concept of the warping degree for twisted knots, construct an invariant for them, and utilize it to establish a labeling scheme for these knots, known as “warping labeling". We have identified that a warping labeling can be extended to twisted virtual braids, enabling the creation of a function that remains invariant under all R-moves except the R2 move. By limiting the labeling set to Z_2, we provide invariants for twisted virtual braids.

Disclaimer: This publication digest may not contain all the papers published. Library has compiled the publication data as per the alerts received from Scopus and Google Scholar for the affiliation “Indian Institute of Technology Ropar” for the month of January, 2026. The author(s) are requested to share their missing paper(s) details if any, for the inclusion in the next publication digest.